Multidimensional random walk for calculating the fusion/fission probabilities of superheavy elements

Aleksander Augustyn
Michał Kowal, Tomasz Cap, Krystyna Siwek-Wilczyńska

NATIONAL CENTRE FOR NUCLEAR RESEARCH
ŚWIERK

25.04.2024
Seminarium Fizyki Jądra Atomowego

Superheavy elements

- Only man-made
- Z>103 (transactinides)
- Produced in nuclear reactions:
  - Cold fusion
  - Hot fusion

IUPAC Periodic Table of the Elements

Key: atomic number / **Symbol** / name / abridged standard atomic weight

1	2	3	4	5	6	7	8	9	10	11	12	13	14	15	16	17	18
1 **H** hydrogen 1.0080 ±0.0002																	2 **He** helium 4.0026 ±0.0001
3 **Li** lithium 6.94 ±0.06	4 **Be** beryllium 9.0122 ±0.0001											5 **B** boron 10.81 ±0.02	6 **C** carbon 12.011 ±0.002	7 **N** nitrogen 14.007 ±0.001	8 **O** oxygen 15.999 ±0.001	9 **F** fluorine 18.998 ±0.001	10 **Ne** neon 20.180 ±0.001
11 **Na** sodium 22.990 ±0.001	12 **Mg** magnesium 24.305 ±0.002											13 **Al** aluminium 26.982 ±0.001	14 **Si** silicon 28.085 ±0.001	15 **P** phosphorus 30.974 ±0.001	16 **S** sulfur 32.06 ±0.02	17 **Cl** chlorine 35.45 ±0.01	18 **Ar** argon 39.95 ±0.16
19 **K** potassium 39.098 ±0.001	20 **Ca** calcium 40.078 ±0.004	21 **Sc** scandium 44.956 ±0.001	22 **Ti** titanium 47.867 ±0.001	23 **V** vanadium 50.942 ±0.001	24 **Cr** chromium 51.996 ±0.001	25 **Mn** manganese 54.938 ±0.001	26 **Fe** iron 55.845 ±0.002	27 **Co** cobalt 58.933 ±0.001	28 **Ni** nickel 58.693 ±0.001	29 **Cu** copper 63.546 ±0.003	30 **Zn** zinc 65.38 ±0.02	31 **Ga** gallium 69.723 ±0.001	32 **Ge** germanium 72.630 ±0.008	33 **As** arsenic 74.922 ±0.001	34 **Se** selenium 78.971 ±0.008	35 **Br** bromine 79.904 ±0.003	36 **Kr** krypton 83.798 ±0.002
37 **Rb** rubidium 85.468 ±0.001	38 **Sr** strontium 87.62 ±0.01	39 **Y** yttrium 88.906 ±0.001	40 **Zr** zirconium 91.224 ±0.002	41 **Nb** niobium 92.906 ±0.001	42 **Mo** molybdenum 95.95 ±0.01	43 **Tc** technetium [97]	44 **Ru** ruthenium 101.07 ±0.02	45 **Rh** rhodium 102.91 ±0.01	46 **Pd** palladium 106.42 ±0.01	47 **Ag** silver 107.87 ±0.01	48 **Cd** cadmium 112.41 ±0.01	49 **In** indium 114.82 ±0.01	50 **Sn** tin 118.71 ±0.01	51 **Sb** antimony 121.76 ±0.01	52 **Te** tellurium 127.60 ±0.03	53 **I** iodine 126.90 ±0.01	54 **Xe** xenon 131.29 ±0.01
55 **Cs** caesium 132.91 ±0.01	56 **Ba** barium 137.33 ±0.01	57-71 lanthanoids	72 **Hf** hafnium 178.49 ±0.01	73 **Ta** tantalum 180.95 ±0.01	74 **W** tungsten 183.84 ±0.01	75 **Re** rhenium 186.21 ±0.01	76 **Os** osmium 190.23 ±0.03	77 **Ir** iridium 192.22 ±0.01	78 **Pt** platinum 195.08 ±0.02	79 **Au** gold 196.97 ±0.01	80 **Hg** mercury 200.59 ±0.01	81 **Tl** thallium 204.38 ±0.01	82 **Pb** lead 207.2 ±1.1	83 **Bi** bismuth 208.98 ±0.01	84 **Po** polonium [209]	85 **At** astatine [210]	86 **Rn** radon [222]
87 **Fr** francium [223]	88 **Ra** radium [226]	89-103 actinoids	104 **Rf** rutherfordium [267]	105 **Db** dubnium [268]	106 **Sg** seaborgium [269]	107 **Bh** bohrium [270]	108 **Hs** hassium [269]	109 **Mt** meitnerium [277]	110 **Ds** darmstadtium [281]	111 **Rg** roentgenium [282]	112 **Cn** copernicium [285]	113 **Nh** nihonium [286]	114 **Fl** flerovium [290]	115 **Mc** moscovium [290]	116 **Lv** livermorium [293]	117 **Ts** tennessine [294]	118 **Og** oganesson [294]

57 **La** lanthanum 138.91 ±0.01	58 **Ce** cerium 140.12 ±0.01	59 **Pr** praseodymium 140.91 ±0.01	60 **Nd** neodymium 144.24 ±0.01	61 **Pm** promethium [145]	62 **Sm** samarium 150.36 ±0.02	63 **Eu** europium 151.96 ±0.01	64 **Gd** gadolinium 157.25 ±0.03	65 **Tb** terbium 158.93 ±0.01	66 **Dy** dysprosium 162.50 ±0.01	67 **Ho** holmium 164.93 ±0.01	68 **Er** erbium 167.26 ±0.01	69 **Tm** thulium 168.93 ±0.01	70 **Yb** ytterbium 173.05 ±0.02	71 **Lu** lutetium 174.97 ±0.01
89 **Ac** actinium [227]	90 **Th** thorium 232.04 ±0.01	91 **Pa** protactinium 231.04 ±0.01	92 **U** uranium 238.03 ±0.01	93 **Np** neptunium [237]	94 **Pu** plutonium [244]	95 **Am** americium [243]	96 **Cm** curium [247]	97 **Bk** berkelium [247]	98 **Cf** californium [251]	99 **Es** einsteinium [252]	100 **Fm** fermium [257]	101 **Md** mendelevium [258]	102 **No** nobelium [259]	103 **Lr** lawrencium [262]

INTERNATIONAL UNION OF PURE AND APPLIED CHEMISTRY

For notes and updates to this table, see www.iupac.org. This version is dated 4 May 2022.

Superheavy elements

Oganessian, Yu. (2006). Synthesis and decay properties of superheavy elements. Pure and Applied Chemistry - PURE APPL CHEM. 78. 889-904. 10.1351/pac200678050889.

- Only man-made
- Z>103 (transactinides)
- Produced in nuclear reactions:
  - Cold fusion
  - Hot fusion

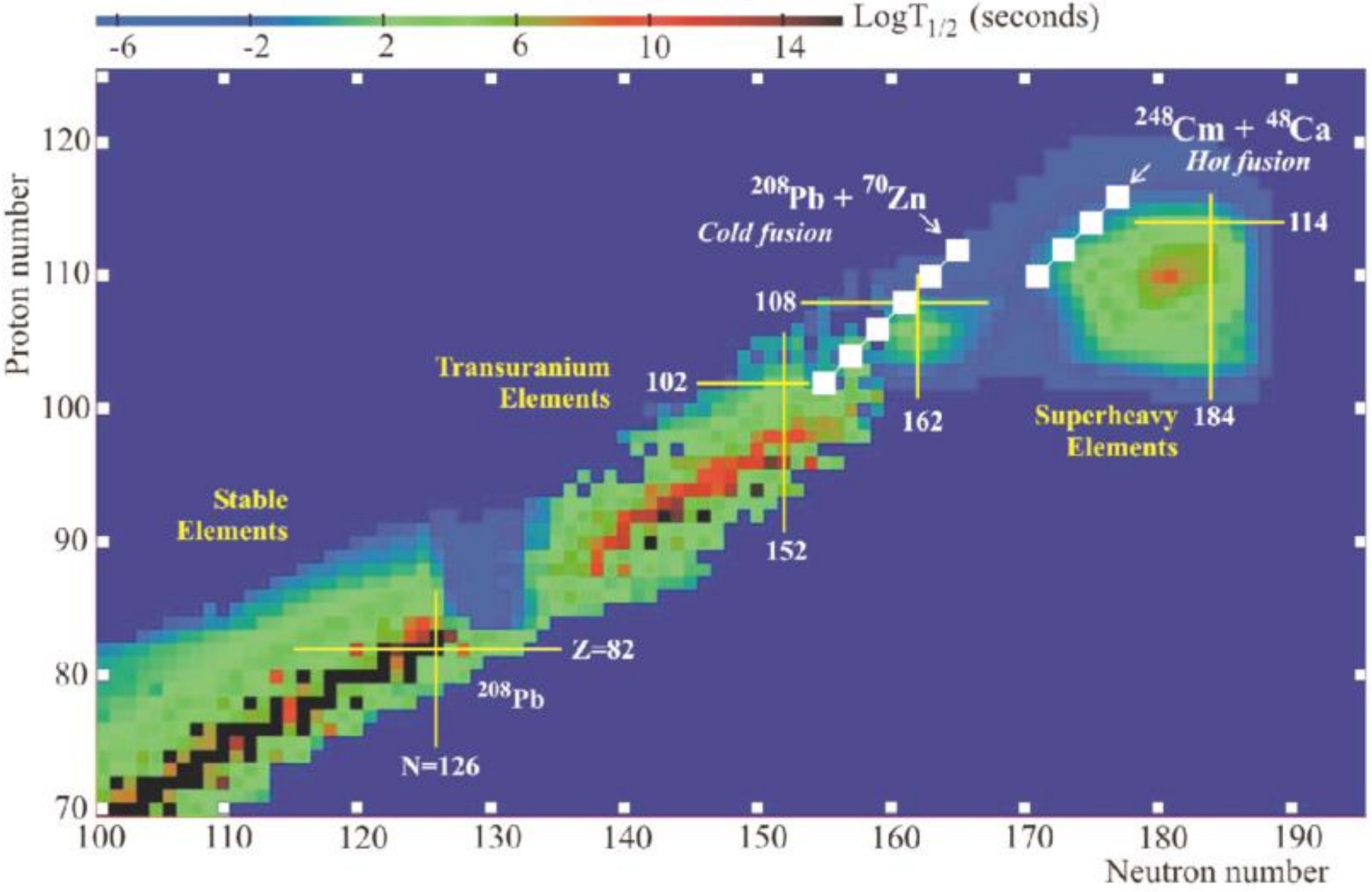

Cold and hot fusion

- $E^* \approx$ 10-20 MeV
- Compound system is only weakly heated and is cooled down via emission of just one or two neutrons
- Magic nuclei as targets (spherical shapes)

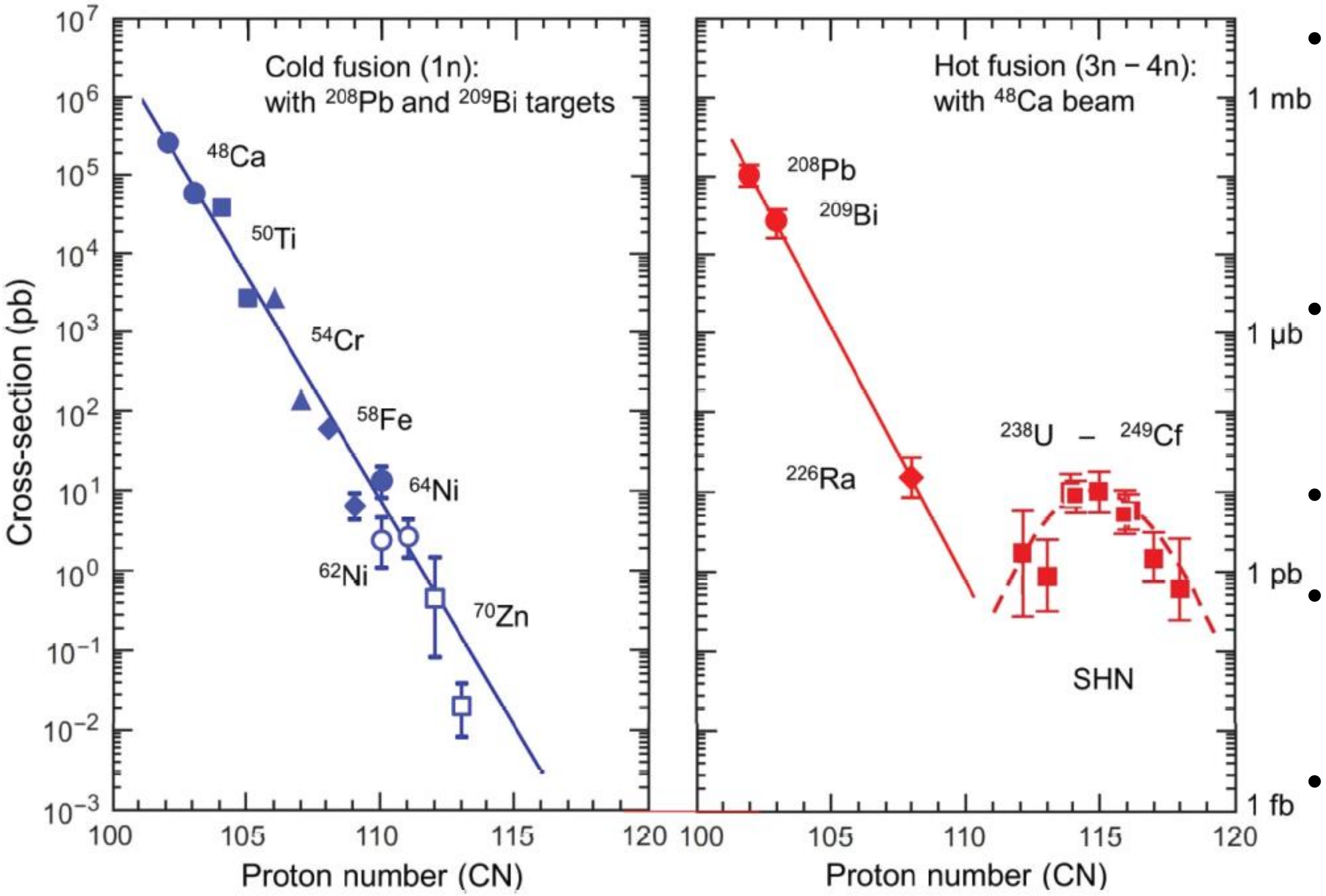

Sigurd Hofmann, Sergey N. Dmitriev, Claes Fahlander, Jacklyn M. Gates, James B. Roberto and Hideyuki Sakai
Report of the 2017 Joint Working Group of IUPAC and IUPAP, Pure Appl. Chem. 2020; 92(9): 1387–1446

- $E^* \approx$ 30-40 MeV
- Compound nucleus is quite excited (most often emits 3 neutrons)
- Well-deformed radioactive actinides (Act.) targets
- Doubly magic projectile ^{48}Ca
- Heavier actinides with Z>98 too short-lived to be used as targets
- Attempts of going beyond the reactions Act. + ^{48}Ca by using heavier projectiles (like ^{50}Ti, ^{54}Cr, ^{58}Fe, ^{64}Ni) gave no results so far.

Motivation

- Experimentalists use theory to determine the optimal reactions and bombarding energies
- A way to calculate P_{fus} would be very helpful in the search for the new elements 119 and 120
- We wanted to use the micro-macro model with the inclusion of rotational energy and a random walk method on potential energy surfaces (PES) to calculate the probability of fusion, while describing the fusion process
- The model is first tested on cold fusion reactions with near spherical projectiles: ^{48}Ca+^{208}Pb, ^{50}Ti+^{208}Pb and ^{54}Cr+^{208}Pb

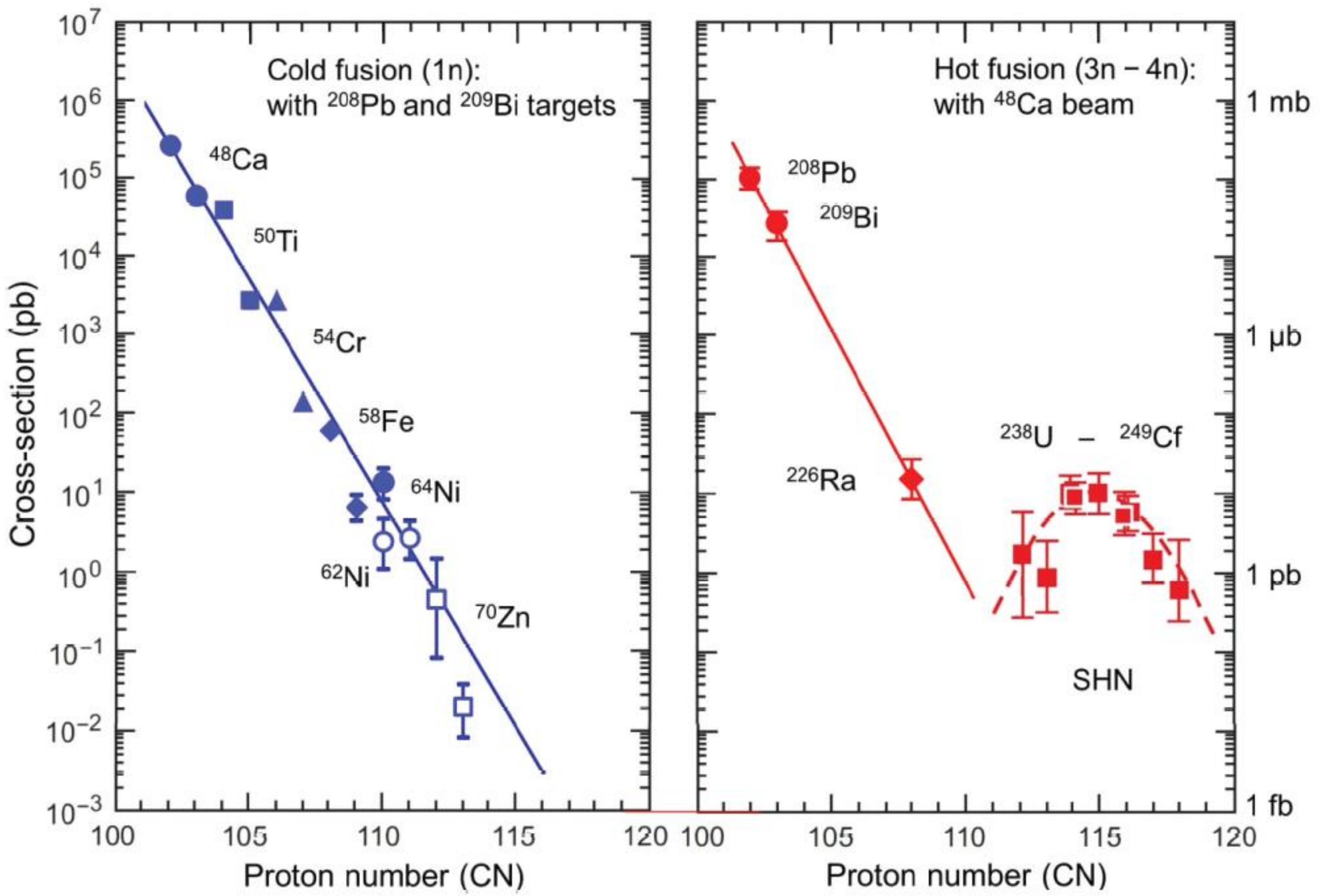

Sigurd Hofmann, Sergey N. Dmitriev, Claes Fahlander, Jacklyn M. Gates, James B. Roberto and Hideyuki Sakai
Report of the 2017 Joint Working Group of IUPAC and IUPAP, Pure Appl. Chem. 2020; 92(9): 1387–1446

Synthesis model

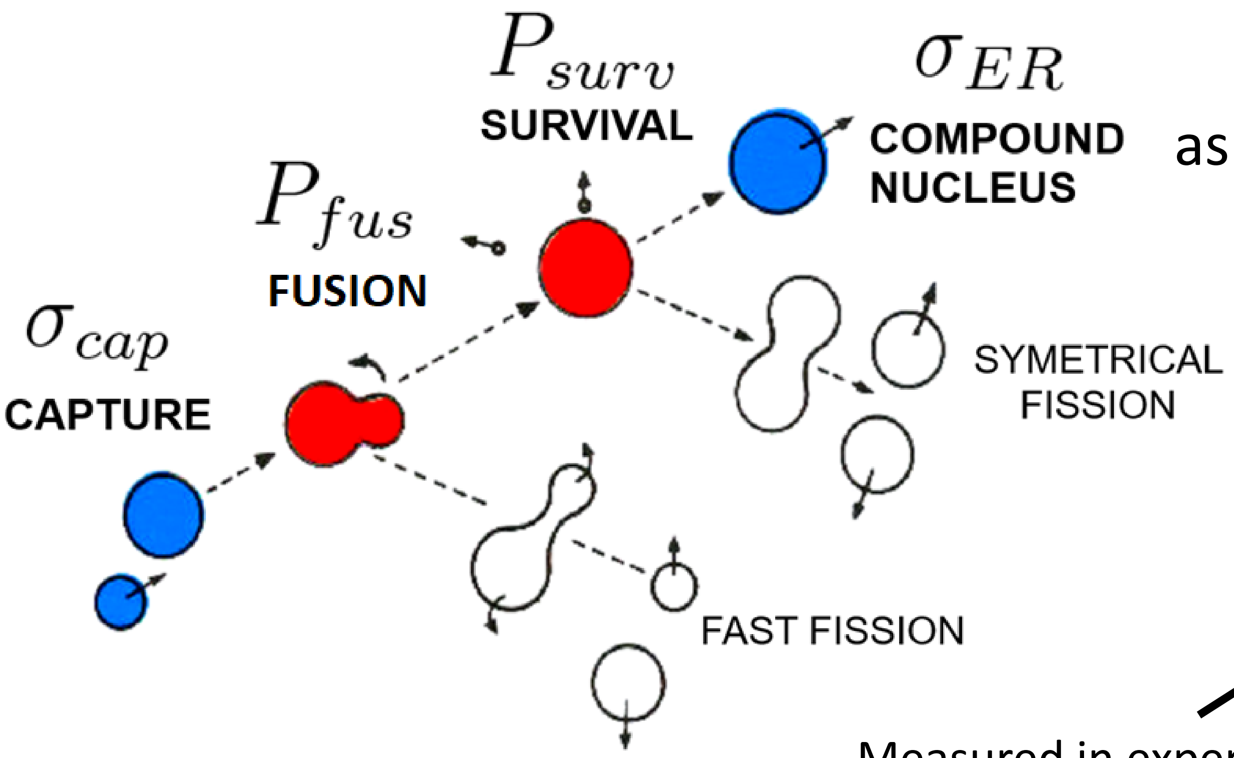

Synthesis of SHN can be described as a **3** step process, due to the different timescales of the particular reaction stages:

$$\sigma_{ER} = \sigma_{cap}\ P_{fus}\ P_{surv}$$

σ_{cap}: Measured in experiments, can be calculated using various models

Diffused barrier formula (Entrance channel barrier is given by a Gaussian distribution)

P_{fus}: Not measured directly, difficult to calculate

Smoluchowski Diffusion Equation, <u>Random Walk</u>

P_{surv}: Well established theory and formulas

Monte Carlo Statistical model

$P_{surv} << 1$

masses, fission barriers, deformations from Warsaw Micro-Macro model

W. J. Świątecki, K. Siwek-Wilczyńska, J. Wilczyński, **PRC 2005**
T. Cap et al., **PRC 2011**
K. Siwek-Wilczyńska et al. **PRC 2012**
T. Cap et al., **PRC 2013**
K. Siwek-Wilczyńska et al. **PRC 2019**

Capture cross section σ_{cap}

- The entrance channel barrier is described by a distribution that can be approximated by a Gaussian function
- The formula for the capture cross section is derived by folding the Gaussian barrier distribution with the classical expression for the fusion cross section

$$\sigma_{cap} = \pi R^2 \frac{\omega}{E_{c.m.}\sqrt{2\pi}}\left[X\sqrt{\pi}(1+\mathrm{erf}(X)) + \exp(-X^2)\right] =$$

$$= \pi \lambda\!\!\!^{-2}(2l_{max}+1)^2, \quad \text{where } X = \frac{E_{c.m.} - B_0}{\omega\sqrt{2}}$$

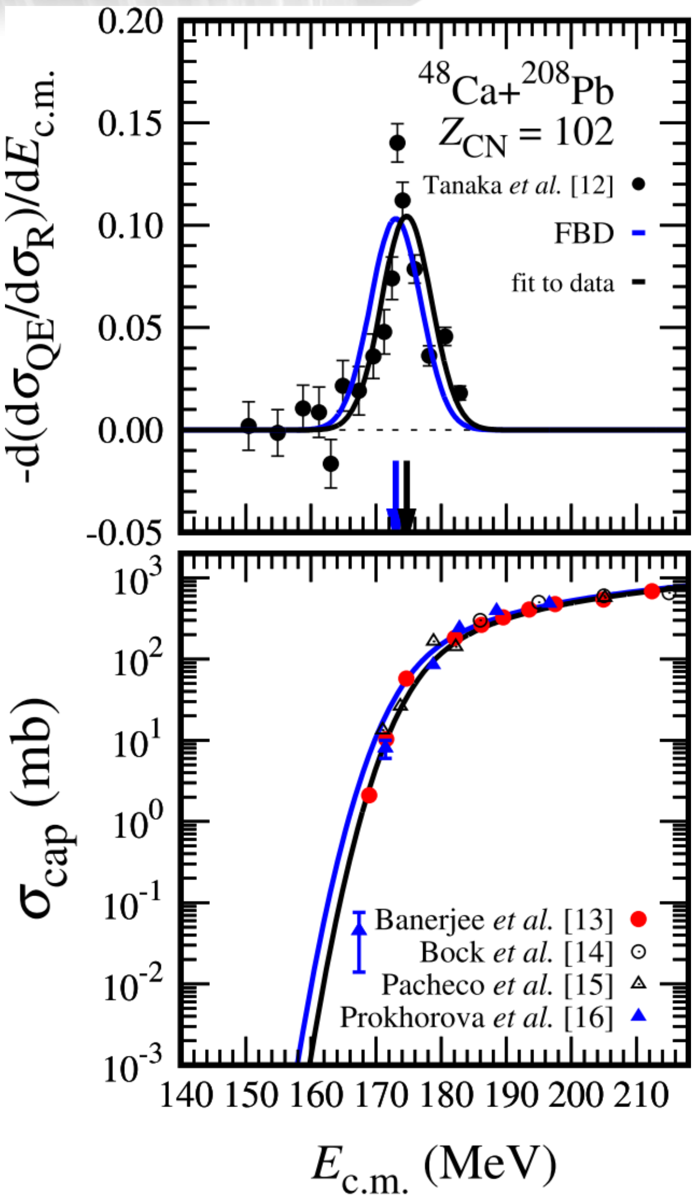

Cap, T., Kowal, M. & Siwek-Wilczyńska, K. The Fusion-by-Diffusion model as a tool to calculate cross sections for the production of superheavy nuclei. *Eur. Phys. J. A* **58**, 231 (2022).

P_{fus} in experiment

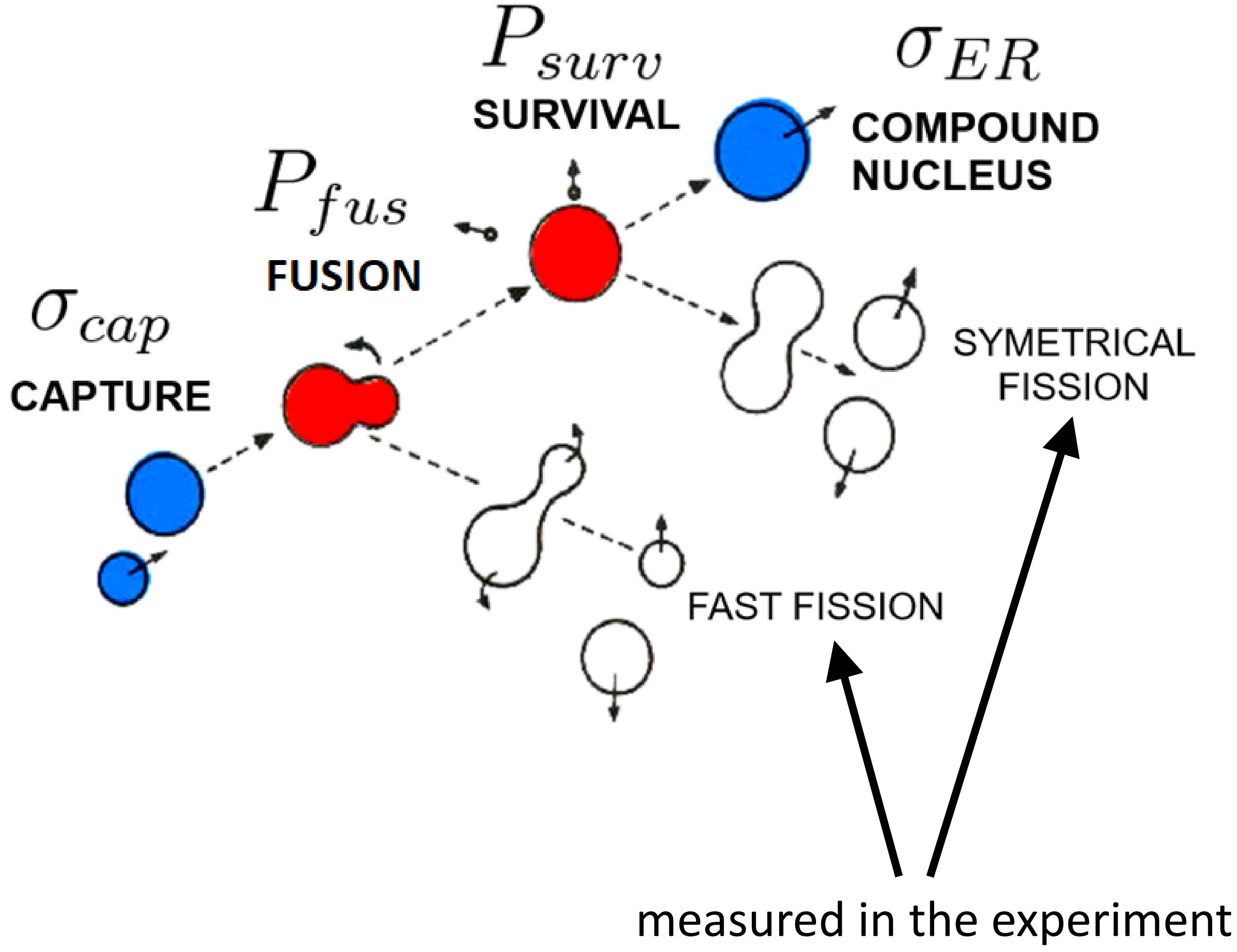

Mechanisms Suppressing Superheavy Element Yields in Cold Fusion Reactions
Banerjee *et al.*, PRL 122, 232503 (2019)

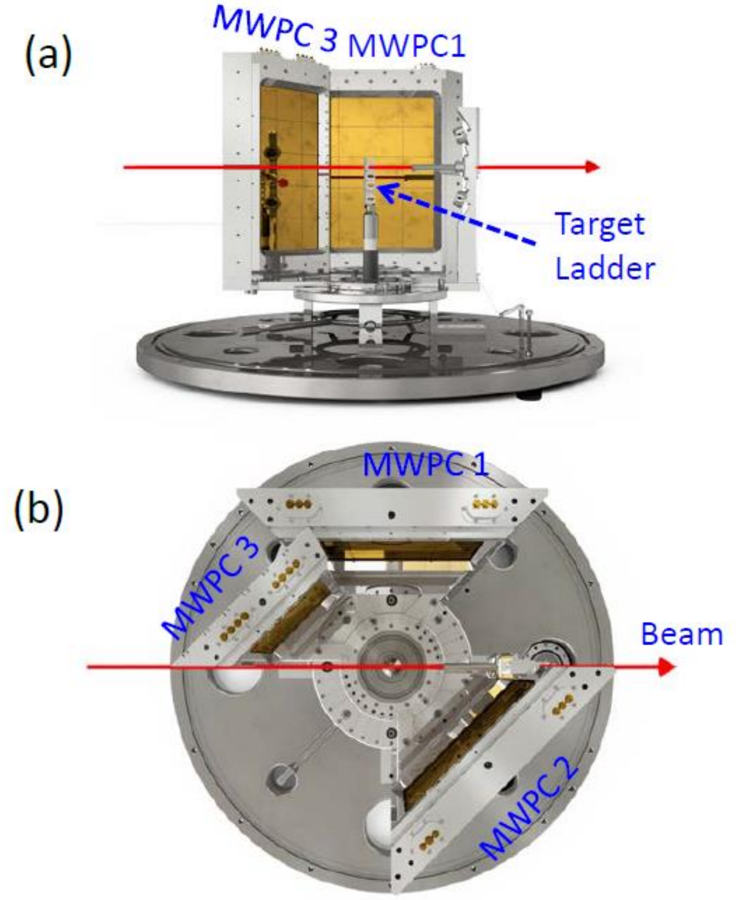

P_{fus} in experiment

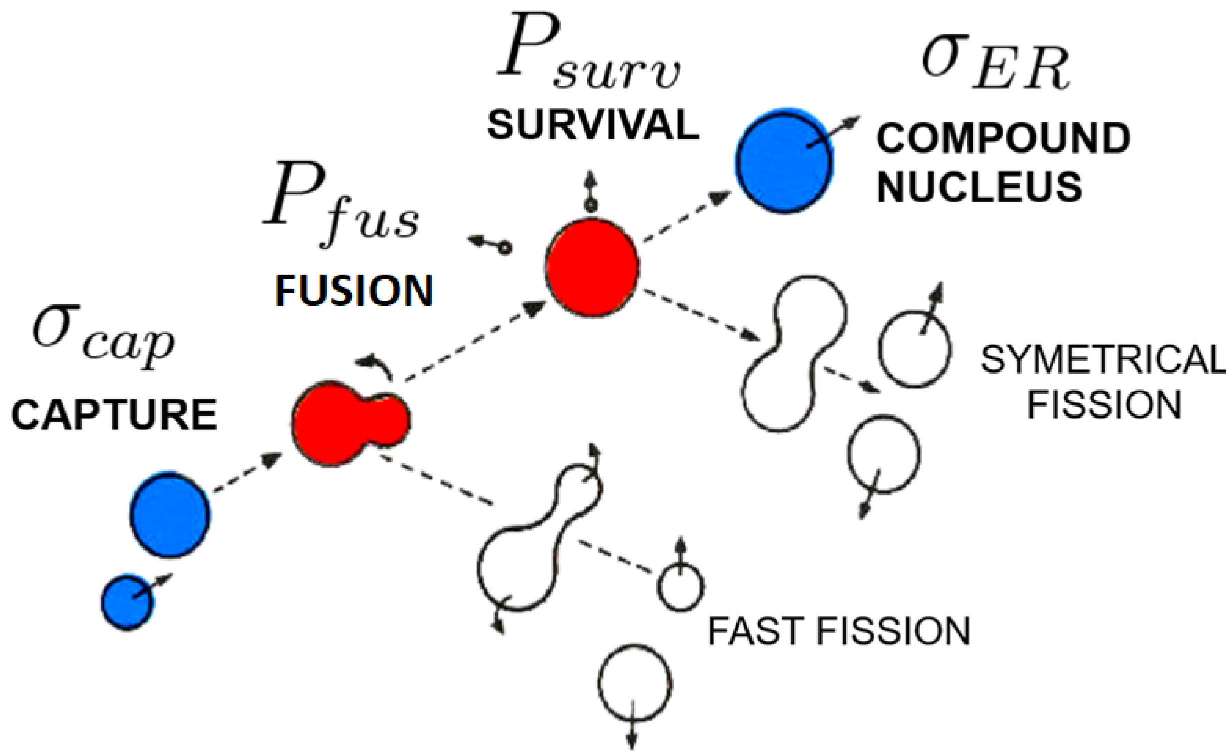

Mechanisms Suppressing Superheavy Element Yields in Cold Fusion Reactions
Banerjee *et al.*, PRL 122, 232503 (2019)

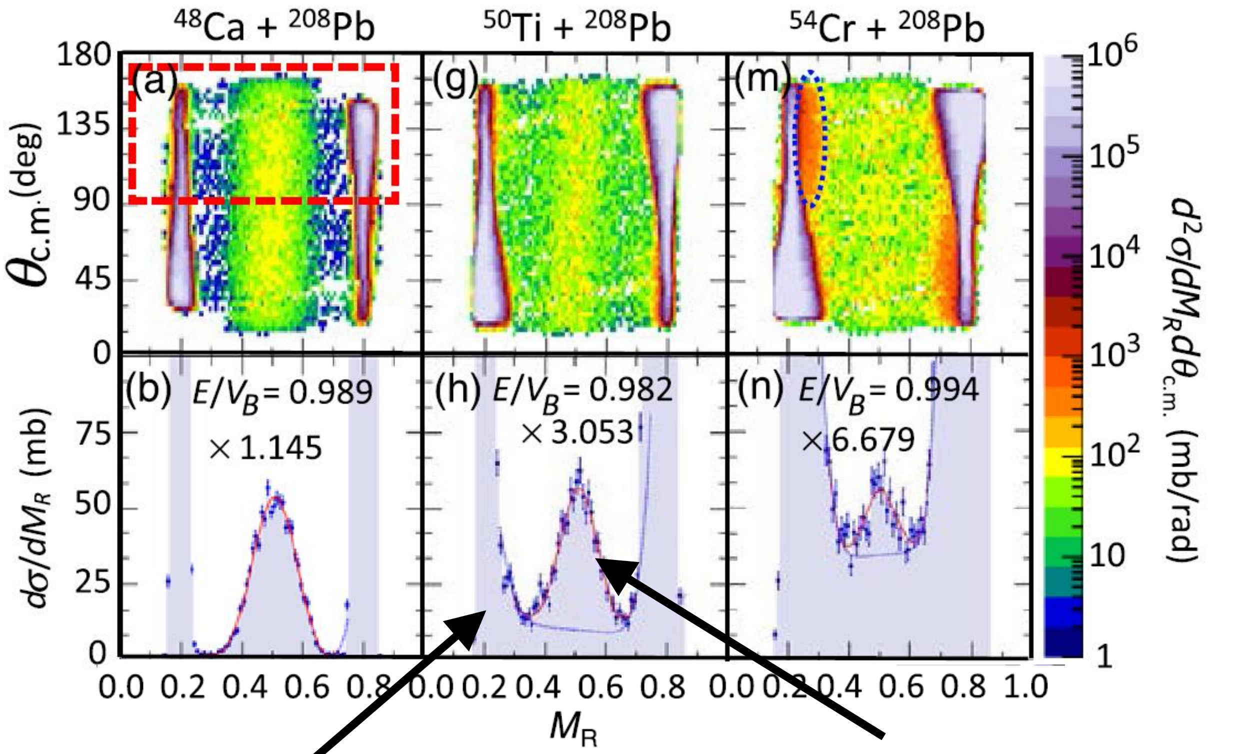

Fast Fission cross section

Mass ratio, Symmetric split: $M_R = 0.5$

Fusion-Fission cross section (symmetrical fission)

P_{fus} can be experimentally estimated:

$$P_{sym} = \frac{\textbf{Fusion–Fission}\text{ cross section}}{\textbf{Capture}\text{ cross section}}$$

Banerjee et al., PRL 122, 232503 (2019)

Reactions:

$^{48}Ca + ^{208}Pb \rightarrow ^{256}No^*$

$^{50}Ti + ^{208}Pb \rightarrow ^{258}Rf^*$

$^{54}Cr + ^{208}Pb \rightarrow ^{262}Sg^*$

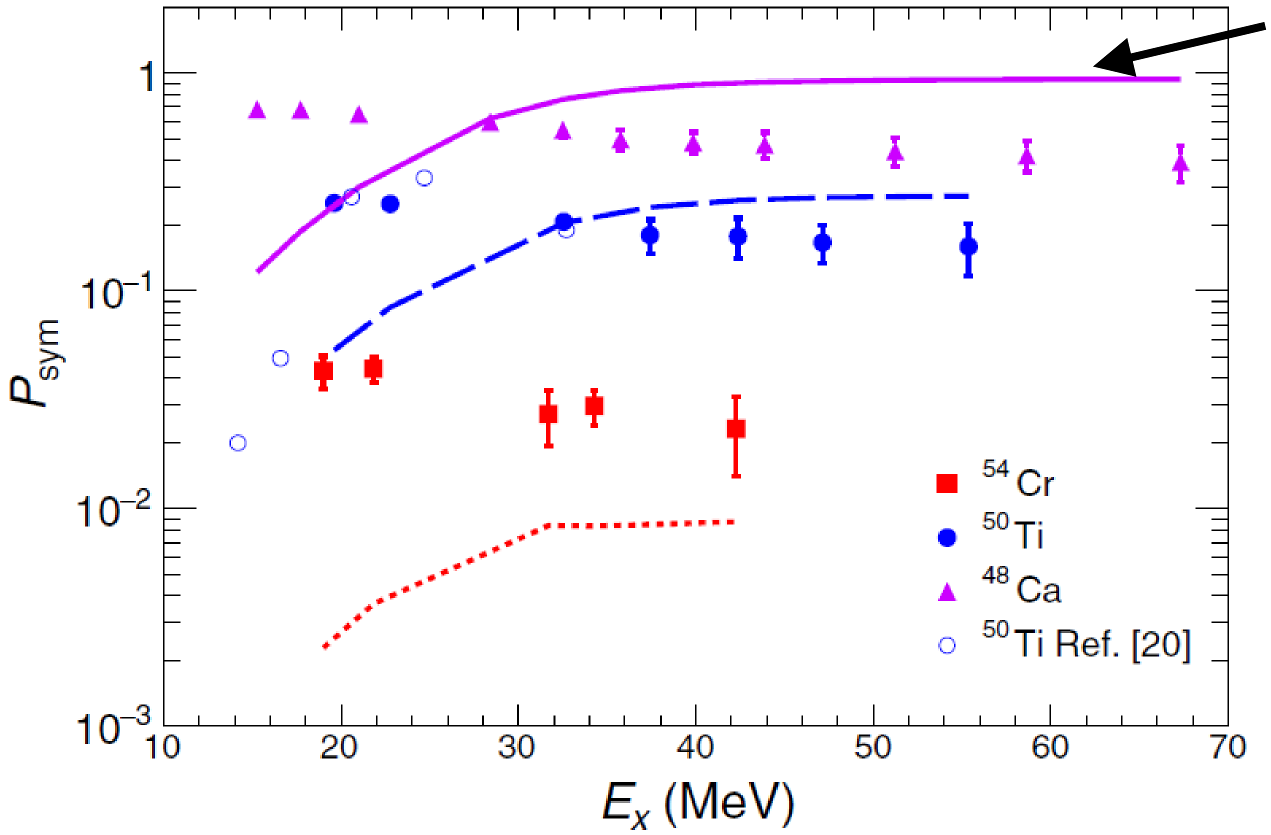

Upper limit for fusion probability

Excitation energy

Diffusion model calculations by V. Zagrebaev and W. Greiner PRC 78, 034610 (2008).

The experimental trends are different than the model predictions for all 3 reactions.

The conclusion was that diffusion is not the main mechanism responsible for the synthesis of SHN.

P_{fus} in Fusion by Diffusion

1D motion approximation
The system must overcome an internal barrier ***H*** to fuse.

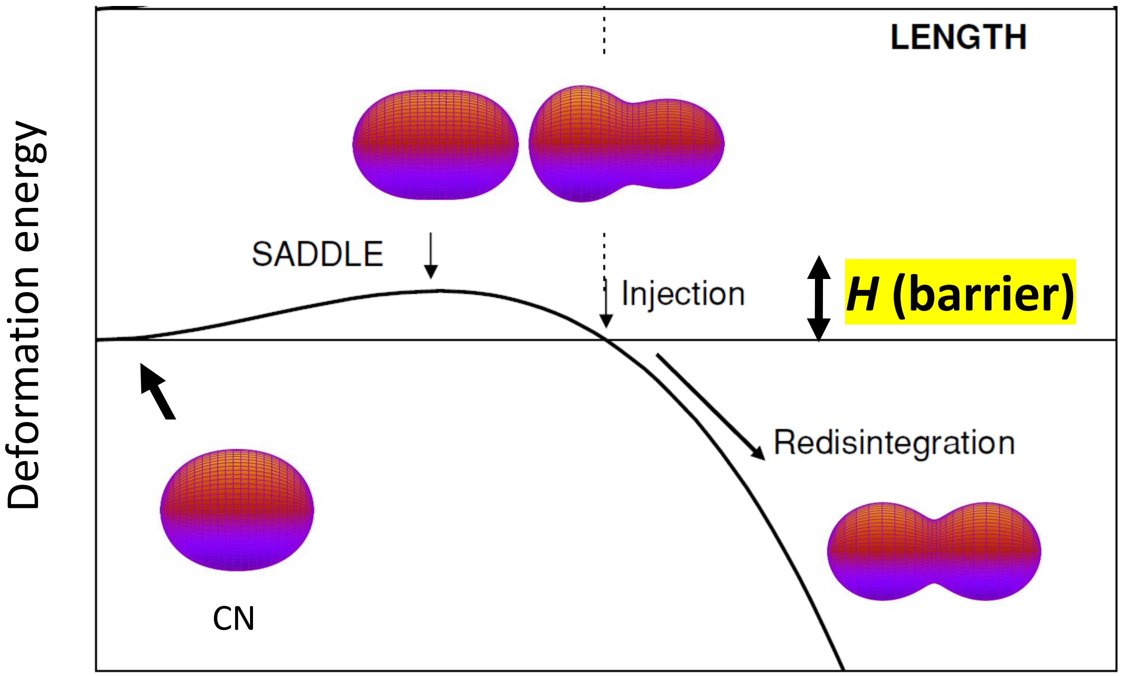

L is the effective elongation (along the fusion path)

P_{fus} is calculated by solving 1D Smoluchowski Diffusion Equation

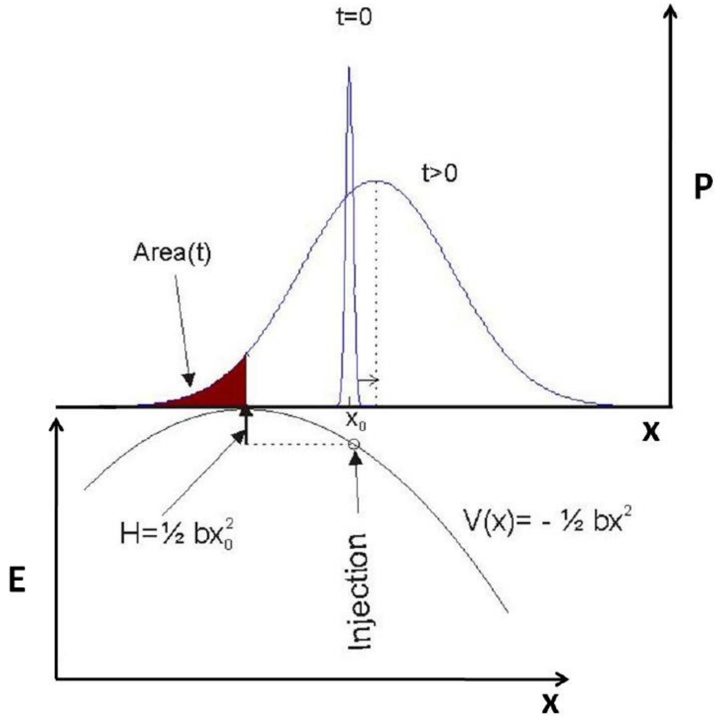

$$P_{fus}(l) = \frac{1}{2}\left(1 - \mathrm{erf}\left(\sqrt{\frac{H(l)}{T}}\right)\right) \text{ when } L_{inj} \geq L_{saddle}$$

H(l) – the function of angular momentum and bombarding energy
T – the temperature depends on available energy

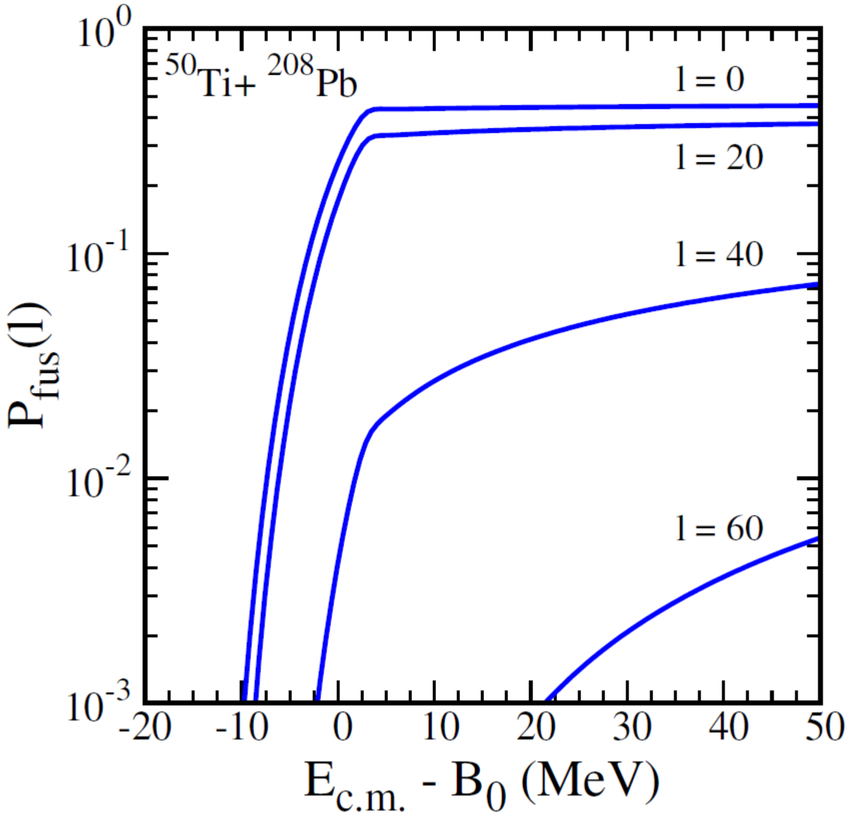

Energy relative to the entrance channel barrier B_0

B_0 = 191.3 MeV

$E^*(E_{c.m.} = B0)$ = 21.7 MeV

l = 0

Central collision

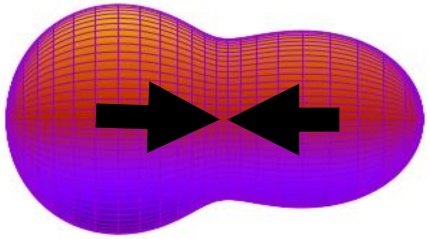

Peripheral collisions

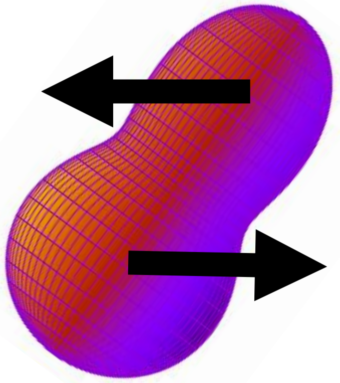

Impact Parameter

Higer partial waves l

=

Higher rotational energy

=

Higher barrier $H(l)$

=

Lower $Pfus(l)$

Fusion probability from FbD model

- Highly effective phenomenological approach
- Only takes into account the macroscopic energy
- Limited to 1 shape dimension

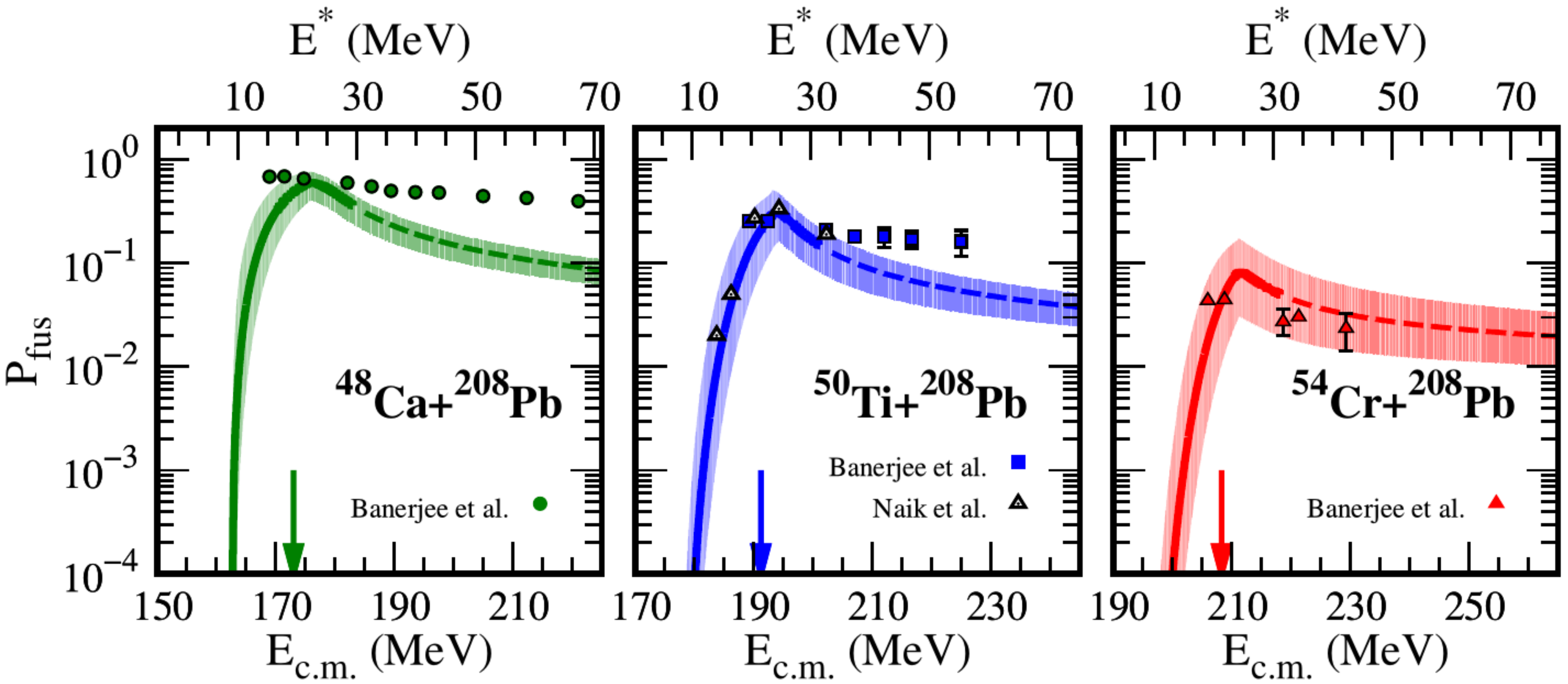

T. Cap, M. Kowal, and K. Siwek-Wilczyńska, Phys. Rev. C **105**, L051601 (2022)

NARODOWE CENTRUM BADAŃ JĄDROWYCH ŚWIERK

Features of the new model

- Using multidimensional deformation space, including the dipole
- Adopting an auxiliary reference frame giving access to otherwise unattainable shapes, specifically the starting configuration
- Adding the shell effect and rotational energy energy to the whole deformation space
- Replacing the Smoluchowski diffusion equation with a biased, unconstrained random walk

Goals of the new model

- Comparison with fragment mass distributions (fission, fusion-fission, quasi-fission) and TKE (total kinetic energy) distributions from experiments
- Study of the competition between fusion-fission and quasi-fission
- Study of the shape evolution during fusion and fission
- Modeling the effect of angular momentum on fusion, fission and quasi-fission
- Prediction of fusion probabilities for new SHE synthesis reactions

Binding/Potential energy in SHE

- Macroscopic (liquid drop) and microscopic (shell effects) energy
- Shell effects responsible for superdeformed minimum in actinides
- SHE exist thanks to the shell effects creating the ground state (often deformed)
- The model needs to account for both energies

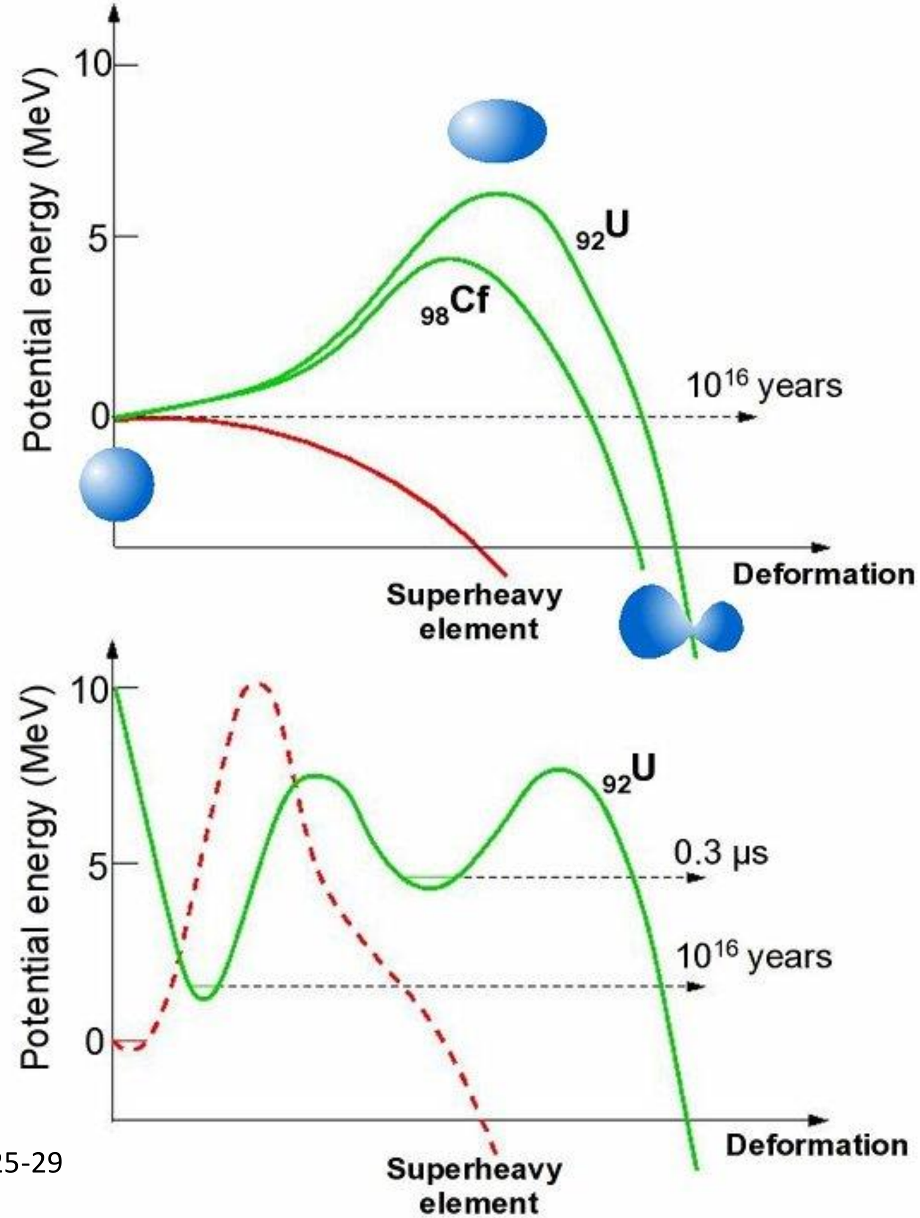

Oganessian, Yu. (2004). Superheavy elements. Physics World, 17(7), 25-29

Atomic Data and Nuclear Data Tables 138 (2021) 101393

Contents lists available at ScienceDirect

Atomic Data and Nuclear Data Tables

journal homepage: www.elsevier.com/locate/adt

Properties of heaviest nuclei with $98 \leq Z \leq 126$ and $134 \leq N \leq 192$

P. Jachimowicz [a], M. Kowal [b,*], J. Skalski [b]

[a] Institute of Physics, University of Zielona Góra, Szafrana 4a, 65-516 Zielona Góra, Poland
[b] National Centre for Nuclear Research, Pasteura 7, 02-093 Warsaw, Poland

Ground-state and saddle-point shapes and masses for 1305 heavy and superheavy nuclei including odd-A and odd–odd systems. Static fission barrier heights, one- and two-nucleon separation energies, and Qα values.

Microscopic–macroscopic method with the deformed Woods–Saxon single-particle potential and the Yukawa-plus-exponential macroscopic energy taken as the smooth part.

Ground-state shapes and energies are found by the minimization over **seven axially-symmetric deformations**.
A search for saddle-points was performed by using the "imaginary water flow" method in three consecutive stages, using five- (for nonaxial shapes) and seven-dimensional (for reflection-asymmetric shapes) deformation spaces.

Good agreement with the experimental data for actinides.

Warsaw macro-micro model

liquid drop with a Yukawa-plus-exponential model

Strutinsky shell correction + Woods-Saxon potential + BCS

$$E_{tot}(Z,N,\beta) = E_{mac}(Z,N,\beta) + E_{mic}(Z,N,\beta)$$

- <u>Allows to obtain the binding energy for a given nuclear shape β</u>
- Macroscopic energy normalized with respect to the sphere:

$$E_{mac} = E_{mac}(deformation) - E_{mac}(sphere)$$

Shape parametrization

- An expansion of the nuclear radius R(θ, ϕ) onto spherical harmonics $Y_{\lambda\mu}(\theta, \phi)$ is used:

$$R(\vartheta,\varphi) = cR_0\{1 + \sum_{\lambda=1}^{\infty} \beta_{\lambda 0} Y_{\lambda 0}(\vartheta,\varphi)\}$$

- For now, shapes in calculations are limited to axially symmetrical (μ = 0)

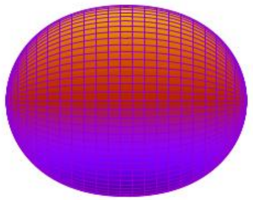

Compound nucleus

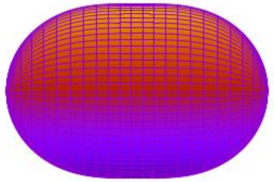

Fission saddle point

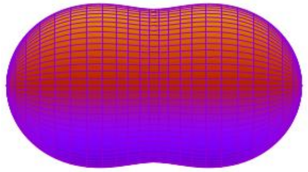

2nd minimum

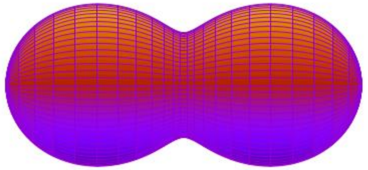

Scission point symmetrical fission

Deformation parameters

- β_{10} – dipole, used as an actual shape parameter
- β_{20} – quadrupole/elongation
- β_{30} – octupole/asymmetry
- β_{40} –hexadecople/neck parameter

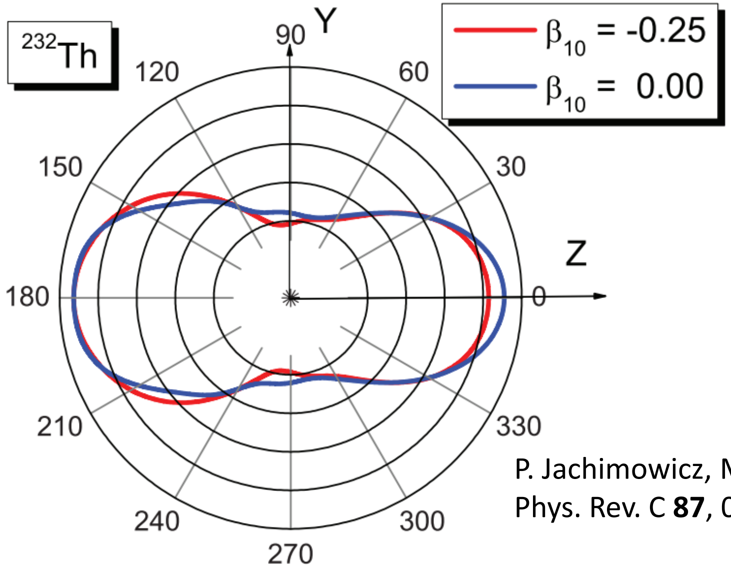

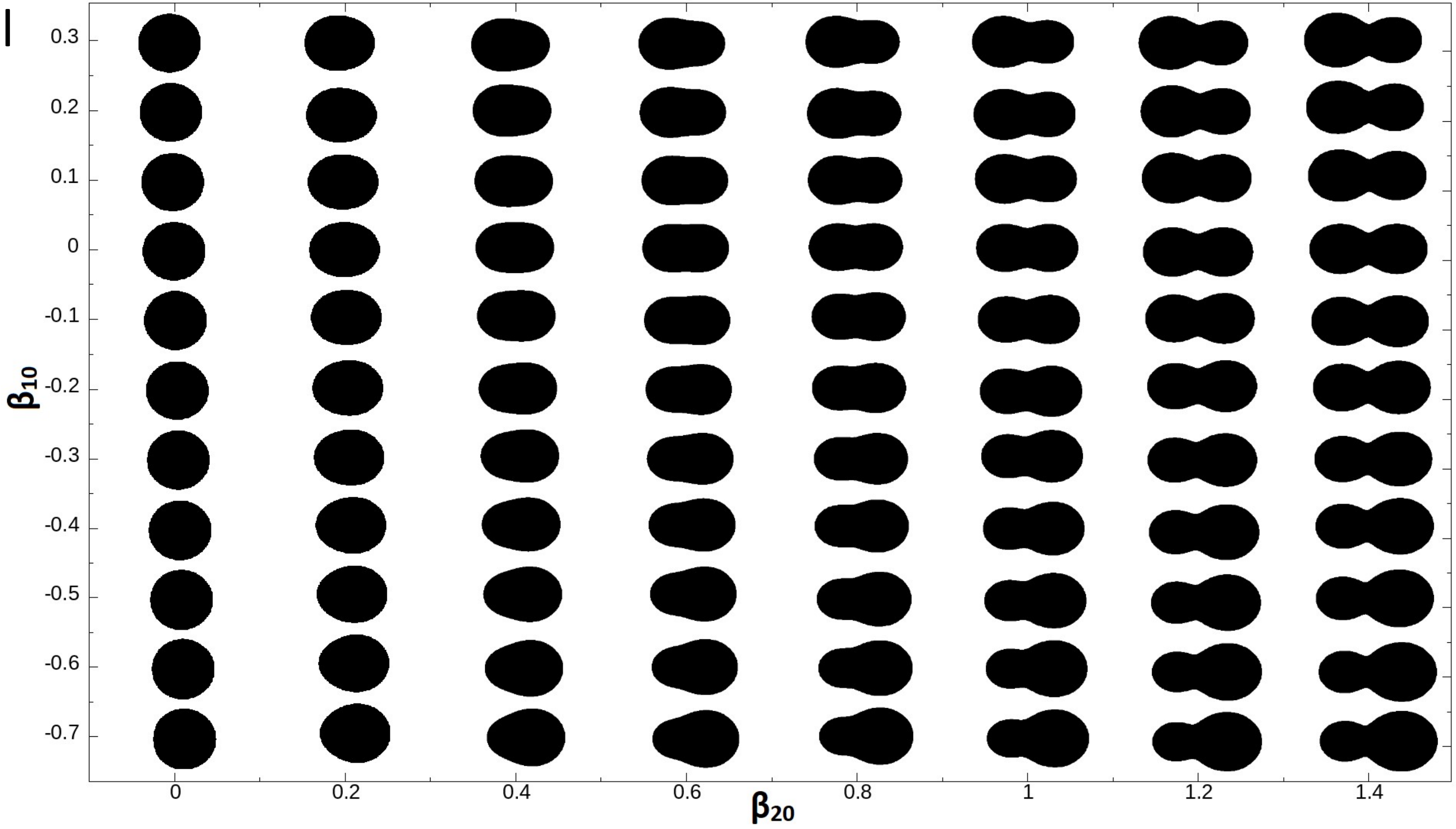

P. Jachimowicz, M. Kowal, and J. Skalski, Phys. Rev. C **87**, 044308 (**2013**)

Potential energy surfaces

- Calculating the energy for a wide array of shapes gives multidimensional potential energy surfaces
- Can be minimized in energy and shown as 3 dimensional maps

$^{48}Ca + ^{208}Pb$

$l = 0$

asymmetry

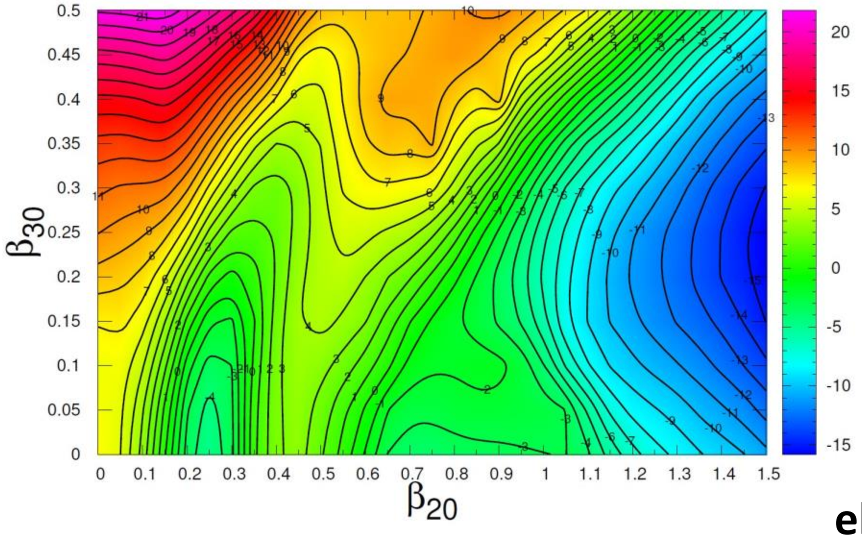

neck parameter

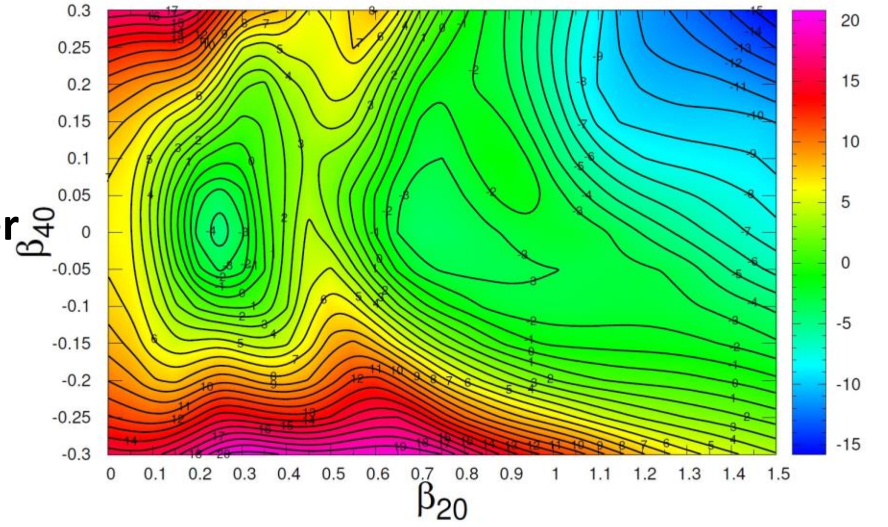

elongation

NARODOWE CENTRUM BADAŃ JĄDROWYCH ŚWIERK

Rotational energy E_{rot}

- Rigid body approximation
- Moment of inertia calculated analytically

$$E_{rot} = l(l+1)\frac{(\hbar c)^2}{2I(\beta)} \qquad \mathbf{I} = \begin{pmatrix} I_\perp & & \\ & I_\perp & \\ & & I_\parallel \end{pmatrix}$$

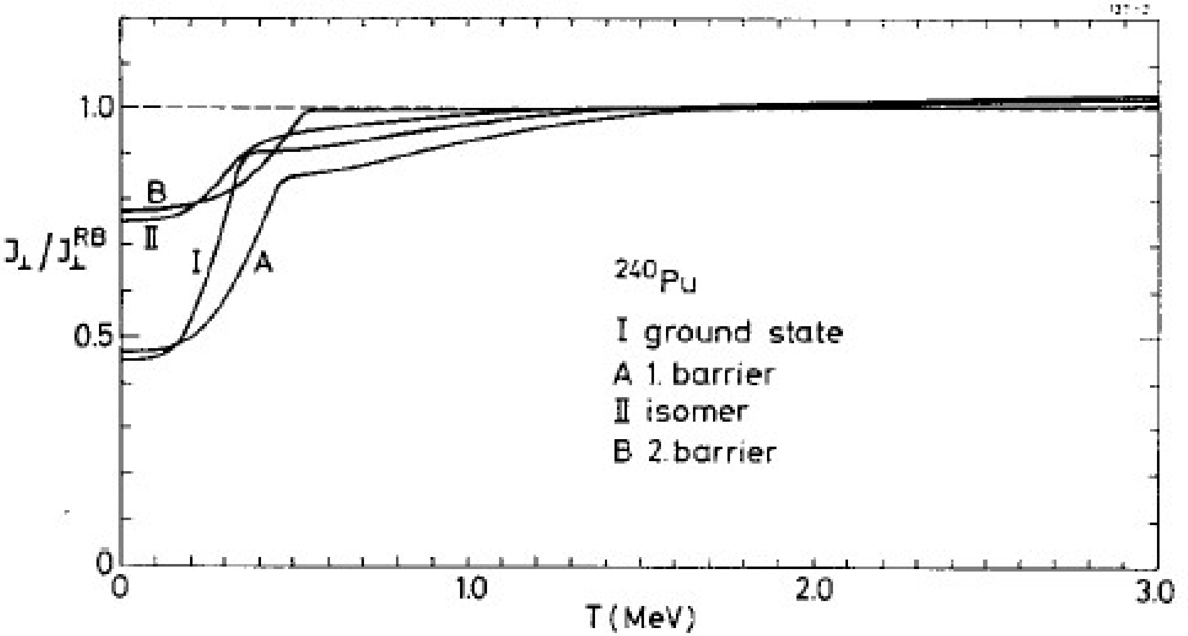

M. Brack, T. Ledergerber, H. Pauli, A. Jensen, Nuclear Physics A **234**, 185–215 (1974)

$$I_\perp = \frac{1}{5}\rho R_0{}^5 \int \sin(\theta)(\pi\sin^2(\theta) + 2\pi\cos^2(\theta))(1 + \frac{1}{2}\sqrt{\frac{3}{\pi}}\beta_{10}\cos(\theta) + \frac{1}{4}\sqrt{\frac{5}{\pi}}\beta_{20}(3\cos^2(\theta) - 1)$$
$$+ \frac{1}{4}\sqrt{\frac{7}{\pi}}\beta_{30}(5\cos^3(\theta) - 3\cos(\theta)) + \frac{1}{16}\sqrt{\frac{9}{\pi}}\beta_{40}(35\cos^4(\theta) - 30\cos^2(\theta) + 3))^5 d\theta$$

Potential energy surfaces with E_{rot}

asymmetry

$^{54}Cr + ^{208}Pb$

$l = 0$

elongation

$^{54}Cr + ^{208}Pb$

$l = 60$

neck parameter

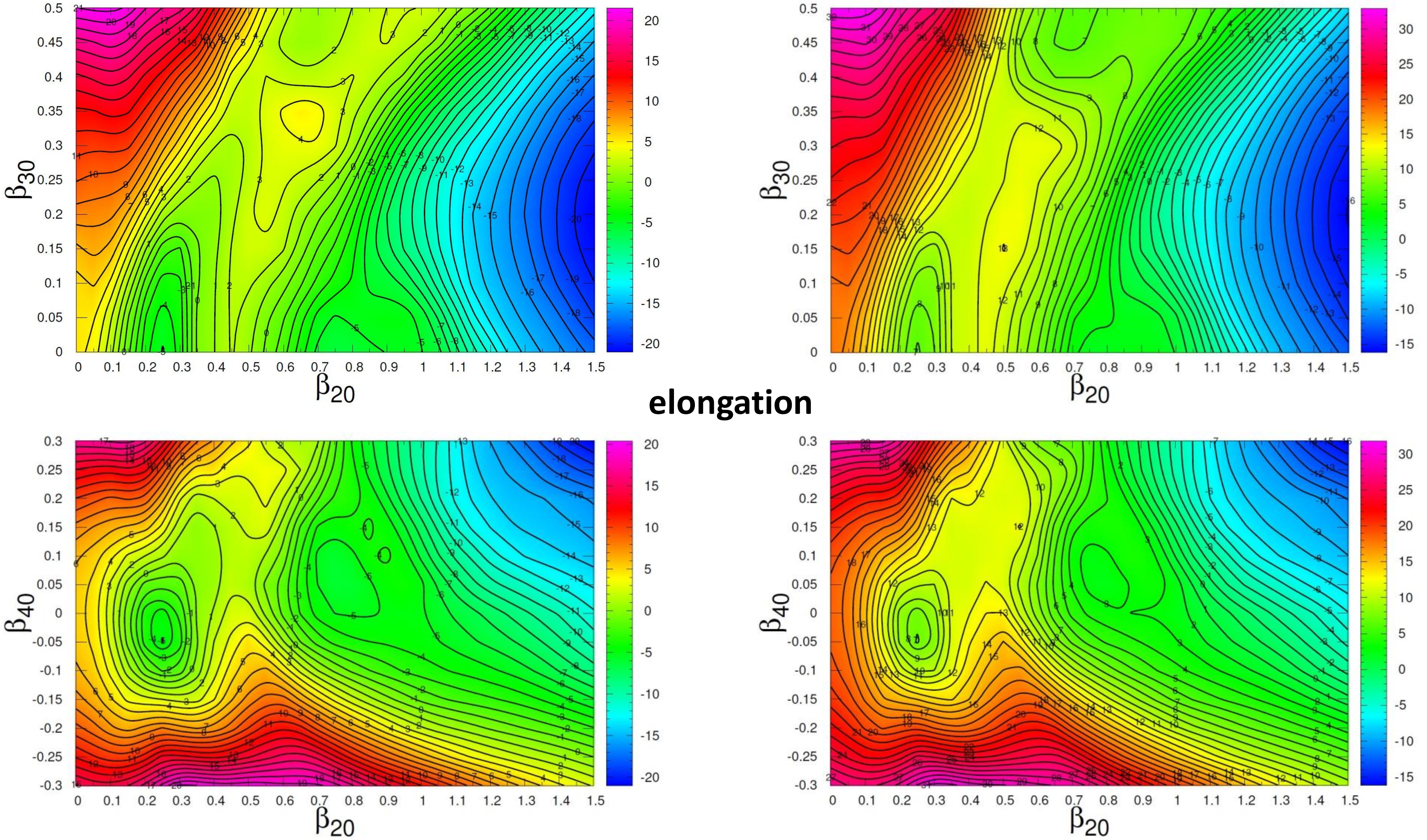

Starting point parametrization

- After overcoming the entrance channel barrier, the projectile and the target are assumed to be spherical and in a touching configuration
- The spherical harmonic parametrization is fitted, with the origin situated in the neck, giving the β parameters for the starting point configuration
- For now calculations are limited to 4 dimensions (β_{10} - β_{40})

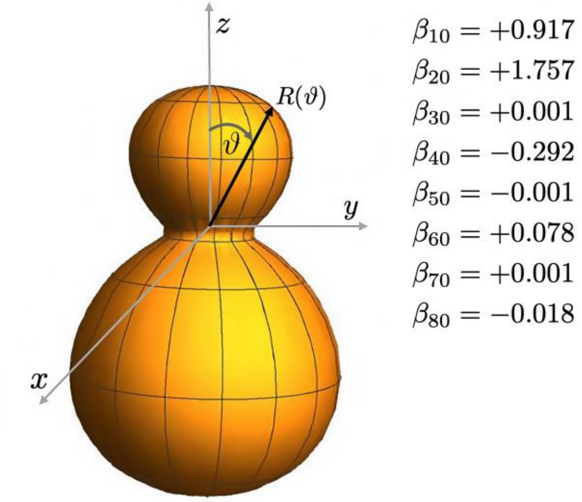

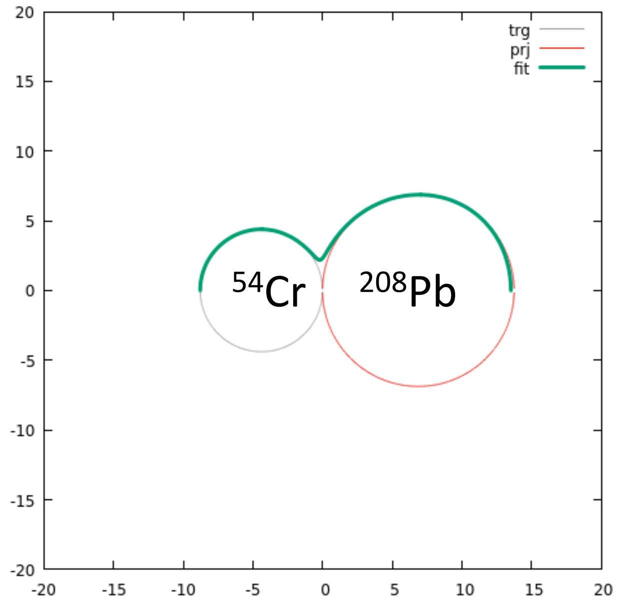

T. Cap, A. Augustyn, M. Kowal, K. Siwek-Wilczyńska, "Dipole-Driven Multidimensional Fusion: An Insightful Approach to the Formation of Superheavy Nuclei", submitted to Phys. Rev. C

NARODOWE CENTRUM BADAŃ JĄDROWYCH ŚWIERK

What do we have?

- We have a parametrization to describe many nuclear shapes
- We can calculate the macroscopic, microscopic and rotational energy for those shapes, giving us PESs for different l values
- We can determine the starting configuration of the fusion process

Now all we need is a way to move on the PESs from one shape to another

$^{48}Ca + ^{208}Pb$

$l = 0$

asymmetry

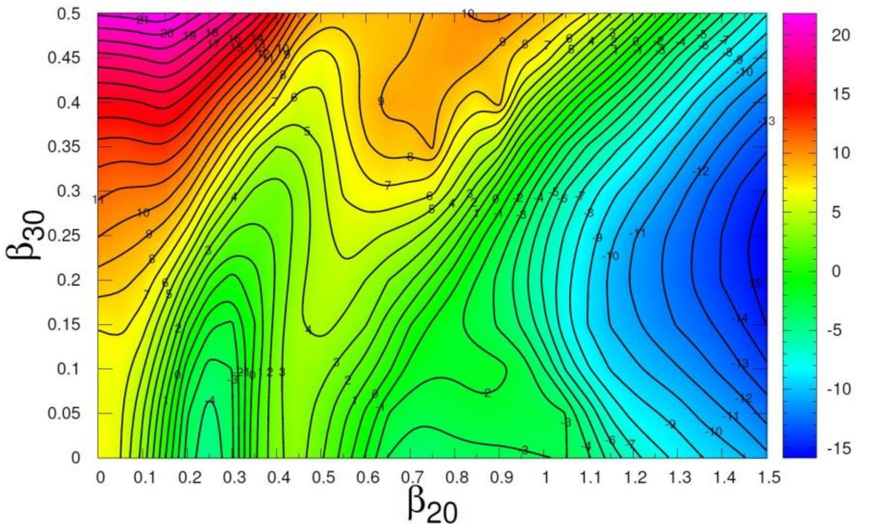

elongation

Biased, unconstrained random walk method

- The probability of transitioning from one shape to another is determined by the number of available energy levels for a given shape β -> biased

$$N_i(\beta_i,\ell) \propto \exp\left(2\sqrt{a\left(E^*_{\max}(\beta_i) - E_{\mathrm{rot}}(\beta_i,\ell)\right)}\right)$$

a – constant density parameter

- Only one β parameter changes at a time, by a step of 0.05, giving 8 possible directions of movement

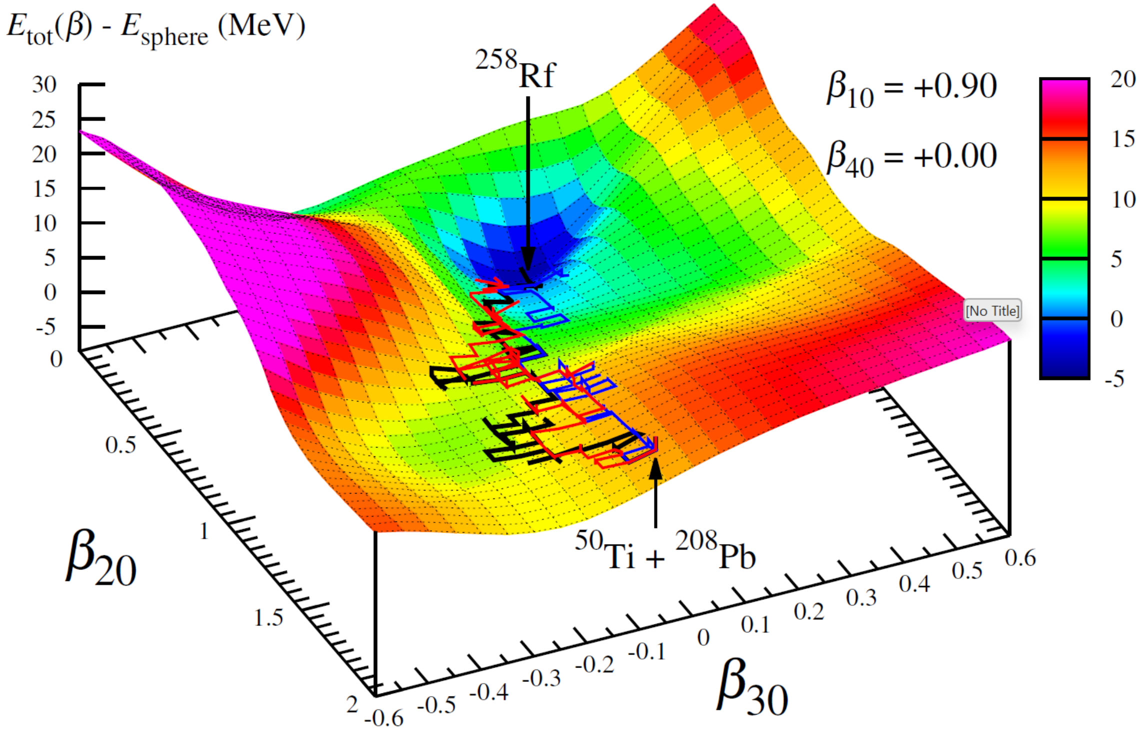

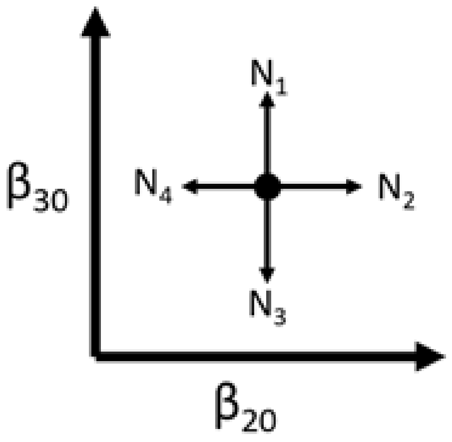

$$P_{i\to j}(\ell) = \frac{N_j(\beta_j,\ell)}{\sum_{k=1}^{8} N_k(\beta_k,\ell)}$$

Biased, unconstrained random walk method

- The random walk occurs in a space where the dimensions β_{20}, β_{30}, and β_{40} are <u>unconstrained</u>, while $|\beta_{10}| < 1.6$.
- The random walk process continues until an end condition is met, either fusion or fission.
- Fusion is reached after crossing the saddle point ($\beta_{20} \leq 0.3$, $|\beta_{30}| \leq 0.2$, and $|\beta_{40}| \leq 0.2$). Splitting occurs when the neck thickness is less than 3 fm.
- Reaching the end condition for a specific collision energy and angular momentum value defines a single path.

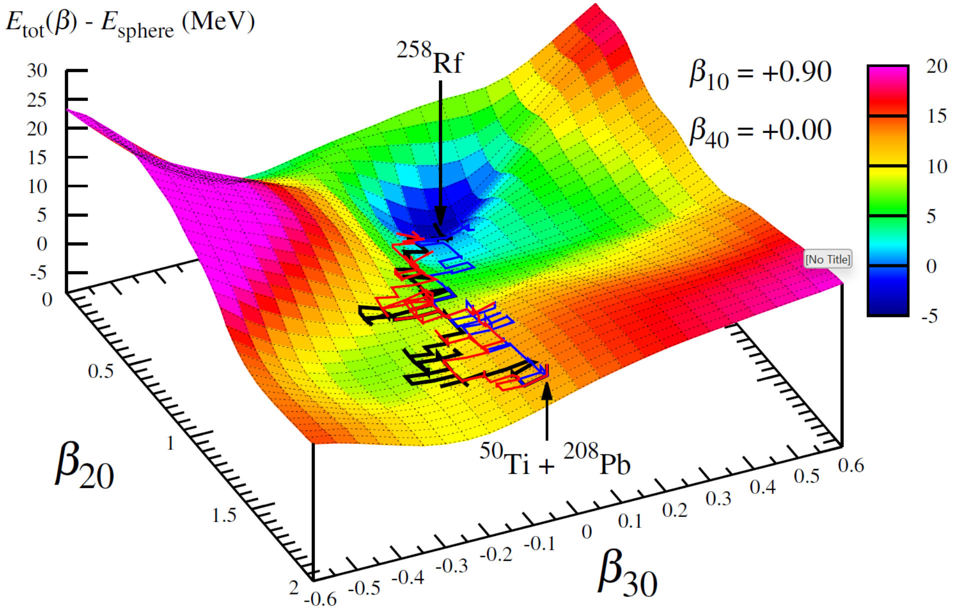

Example of a paths

$^{54}Cr + ^{208}Pb$

$E^* = 50$ MeV, $l = 40$

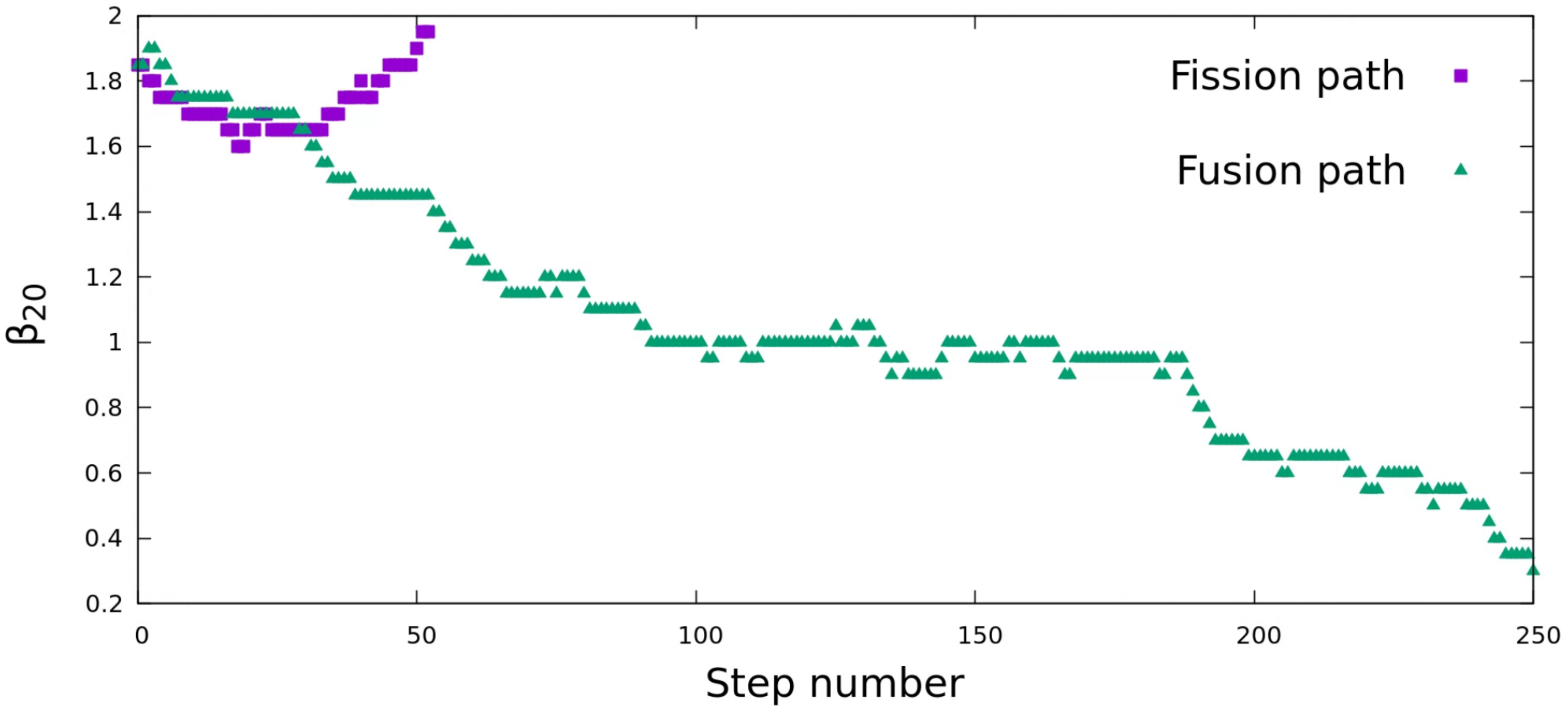

Example of a paths

$^{54}Cr + ^{208}Pb$

$E^* = 50$ MeV, $l = 40$

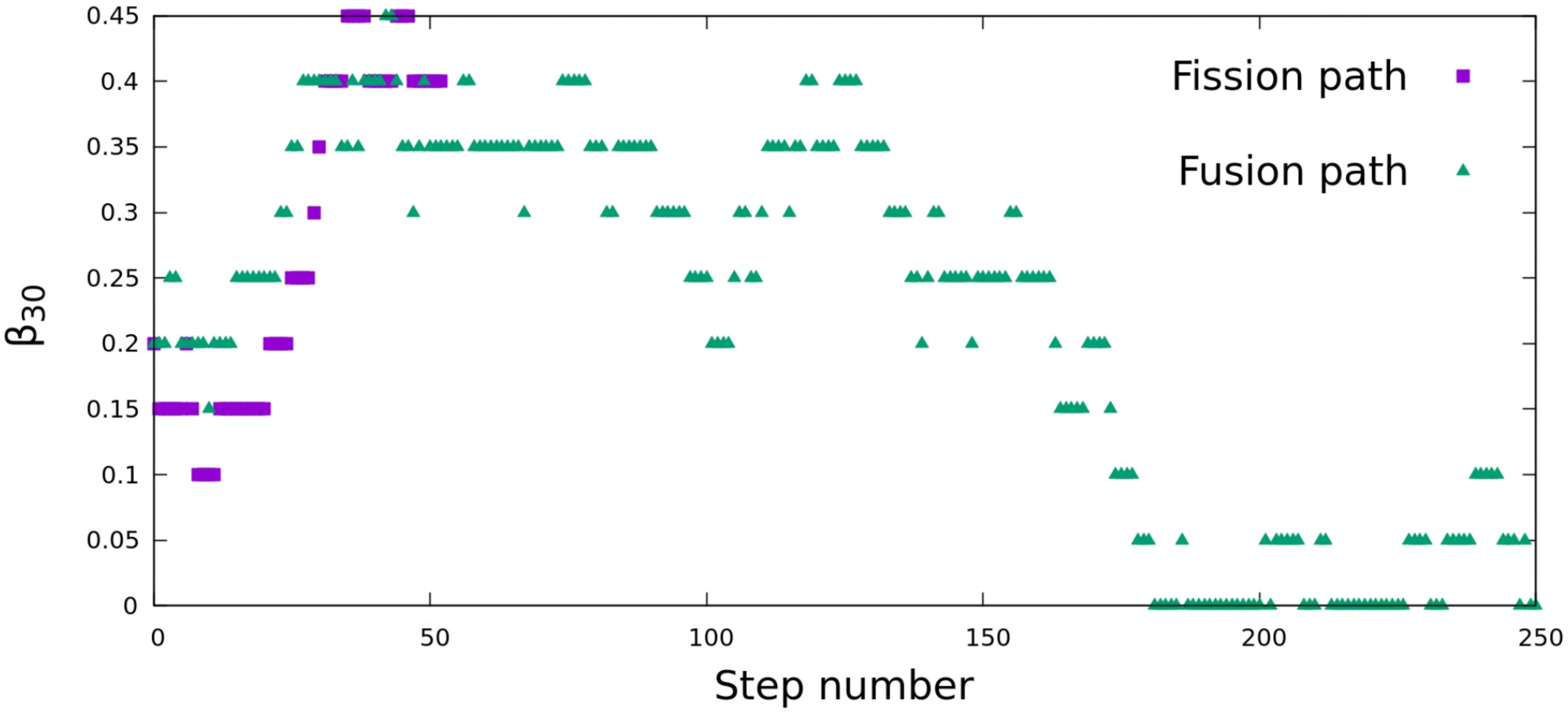

Example of a paths

$^{54}Cr + ^{208}Pb$

$E^* = 50$ MeV, $l = 40$

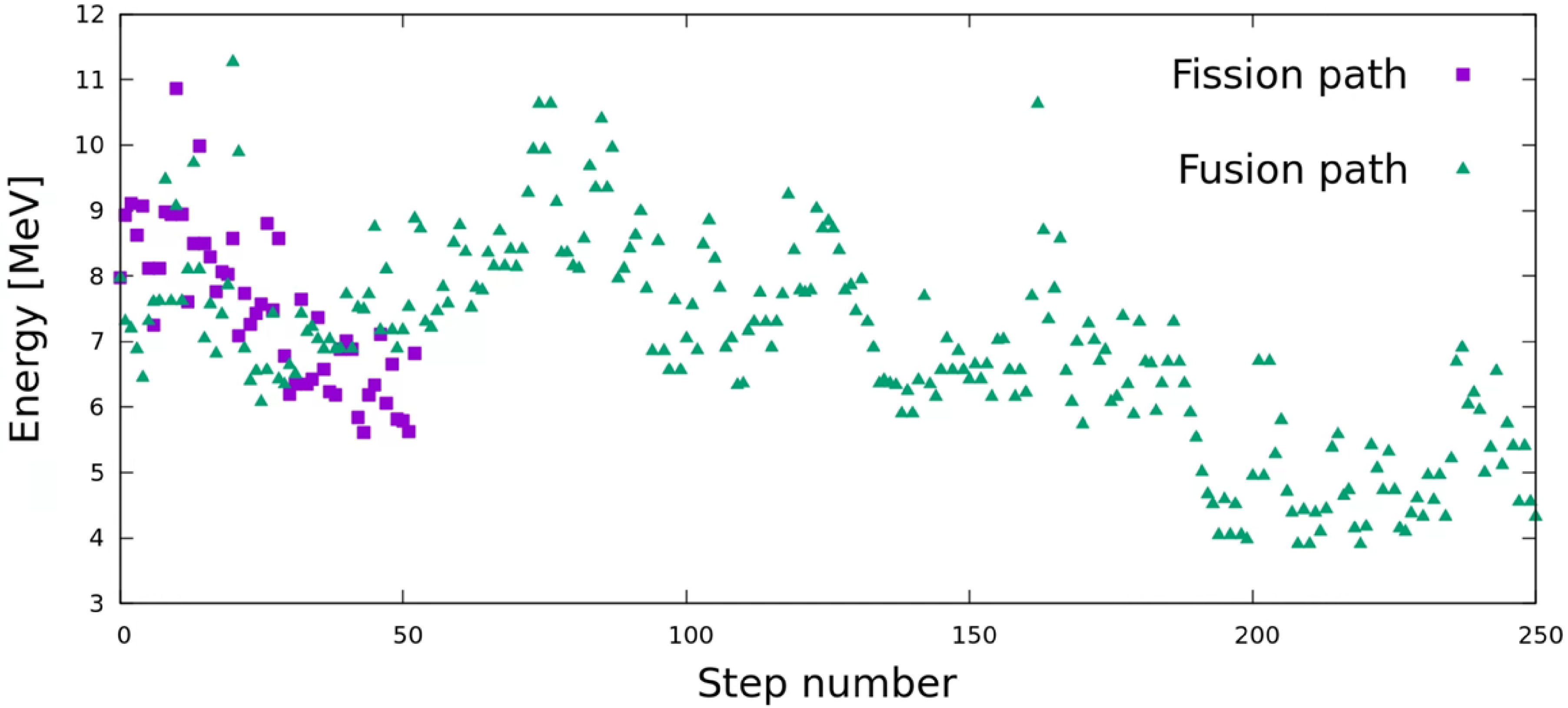

NARODOWE CENTRUM BADAŃ JĄDROWYCH ŚWIERK

Biased, unconstrained random walk method

- Calculations were done for excitation energies from 15 to 70 MeV with 1 MeV step. 10^5 paths were calculated for a given energy and l-value from 0 to l_{max}. $P_{fus}(E_{cm}, l)$ is given as a ratio of the number of paths that lead to fusion to the total number of paths

$$P_{fus}(E_{cm}, l) = \frac{\text{paths which ended in fusion}}{10^5}$$

- ~ 3000 E^* and l combinations → ~300 million paths per reaction

Capture and fusion cross section

- Capture cross section calculated from FbD model
- Fusion cross section from the random walk method $\sigma_{fus} = \pi \lambda^2 \sum_{l=0}^{l_{max}} (2l+1) T(l) P_{fus}(l) = \sigma_{cap} \times P_{fus}$
- Distributions of $\frac{d\sigma_{cap}}{dl}$ (black) and $\frac{d\sigma_{fus}}{dl}$ (red) for $^{48}Ca + {}^{208}Pb$

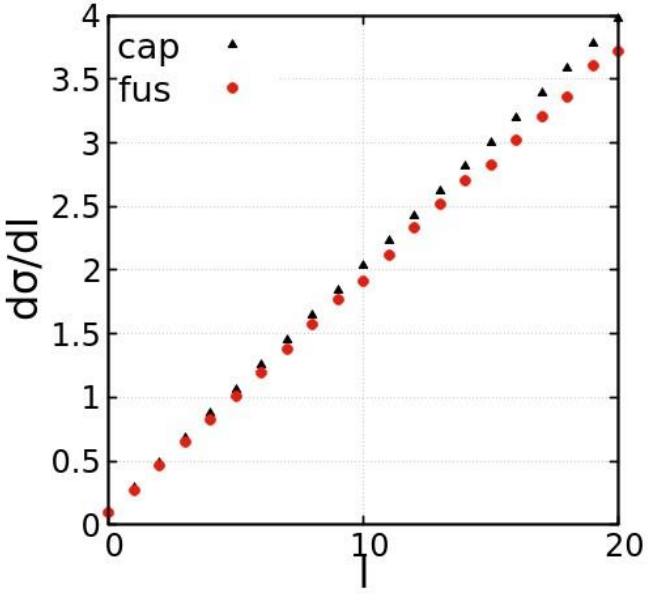

$E^* = 20$ MeV

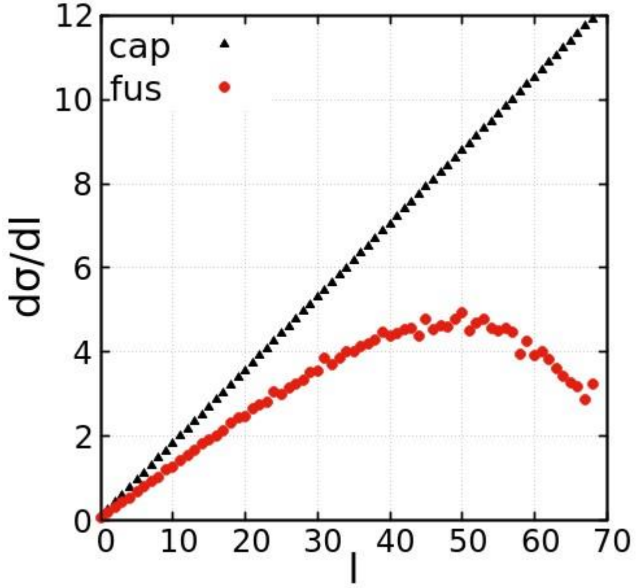

$E^* = 40$ MeV

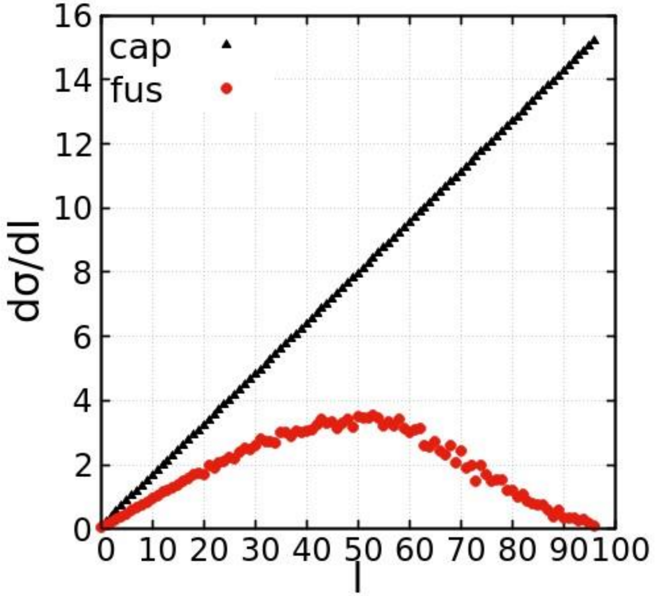

$E^* = 60$ MeV

Fusion probability from the random walk

Average over l to get P_{fus} dependant on E_{cm}: $P_{fus}(E_{cm}) = \frac{\sum_{l=0}^{lmax}(2l+1)P_{fus}(l)}{(2l_{max}+1)^2}$ fusion probability averaged over l

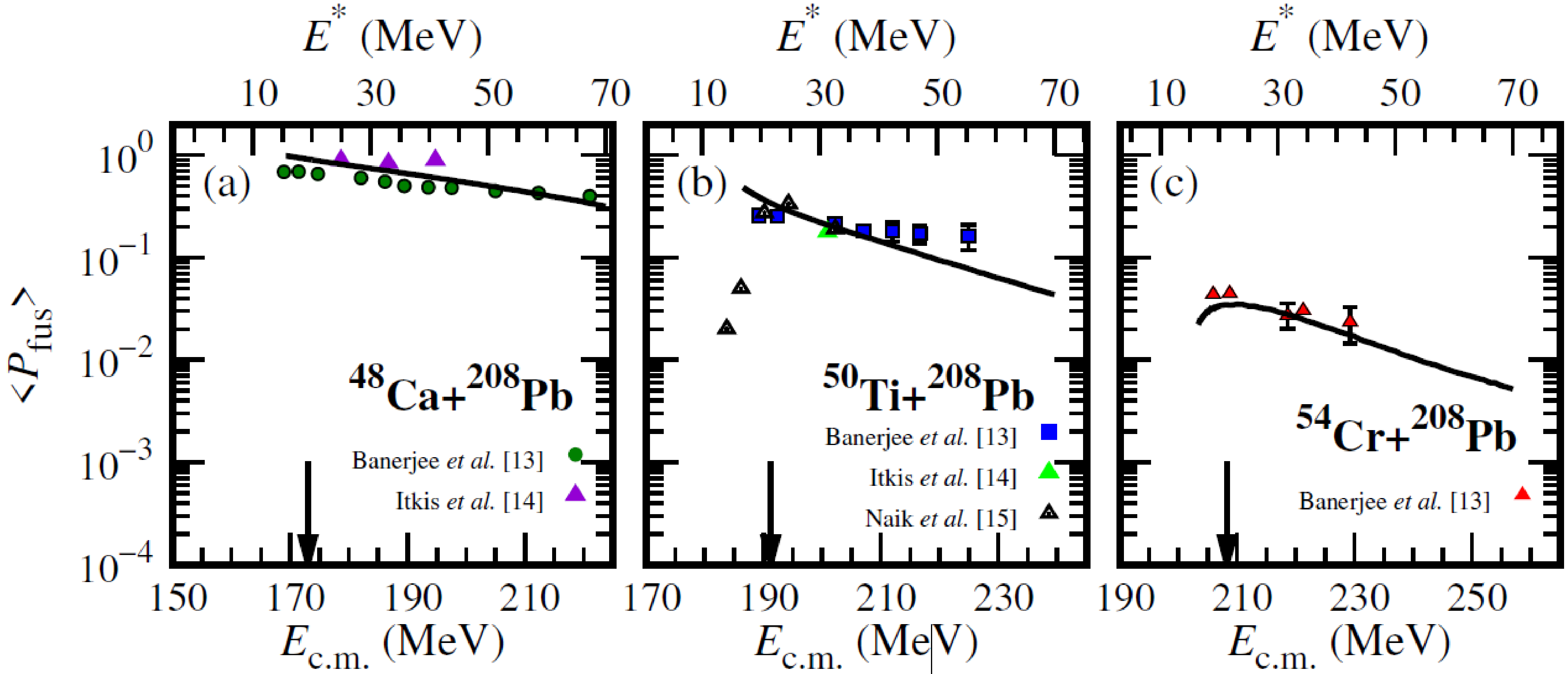

The averaged fusion probabilities < Pfus > (solid black lines) calculated using the random walk method for the $^{48}Ca+^{208}Pb$, $^{50}Ti+^{208}Pb$, and $^{54}Cr+^{208}Pb$ reactions. Experimental data are taken from [K. Banerjee et al., PRL 122, 232503 (2019)], [M. Itkis et al., EPJ 58, 178 (2022] and [R. S. Naik et al., PRC 76, 054604 (2007)] The arrows represent the locations of the mean entrance channel barrier B_0 for each reaction.

NARODOWE CENTRUM BADAŃ JĄDROWYCH ŚWIERK

Mass distribution of fission fragments

- The final fission shapes can be divided, and their volumes compared, giving the mass distribution of fission fragments, for each E* and *l*.

$^{54}Cr + ^{208}Pb$

*E** = 30 MeV, *l* = 20

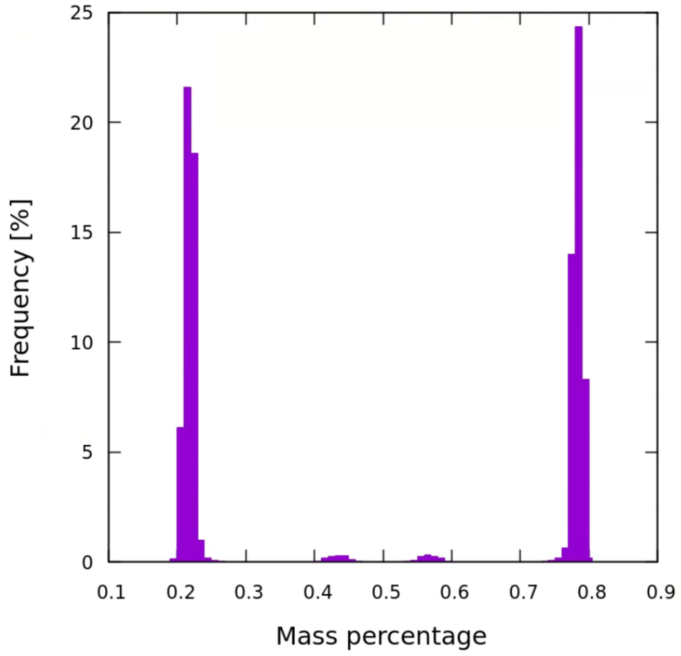

$^{54}Cr + ^{208}Pb$

*E** = 50 MeV, *l* = 40

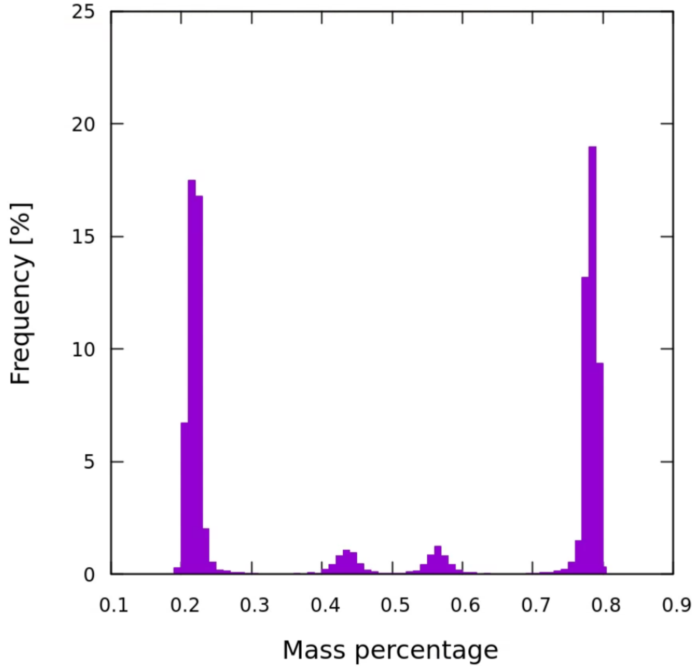

$^{54}Cr + ^{208}Pb$

*E** = *70* MeV, *l* = 70

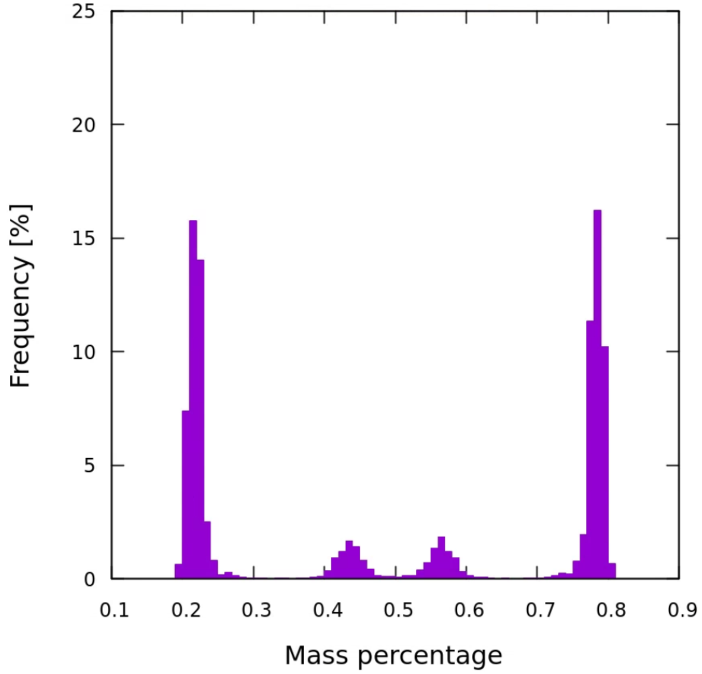

Next steps for fusion

- Expand to 8 $\beta_{\lambda 0}$ dimensions
- Determine optimal step size for each β parameter
- Expand the model to describe under barrier reactions
- Expand to non-axially symmetric shapes ($\beta_{\lambda\mu}$) and incorporate multiple possible starting points depending on the orientation of the target and the projectile
- Introduce a density parameter beyond Fermi gas model and incorporate shell-correction damping
- Allow for the emission of neutrons, protons and alfa particles during the random walk

Emission of neutrons, protons and alfa particles during the random walk

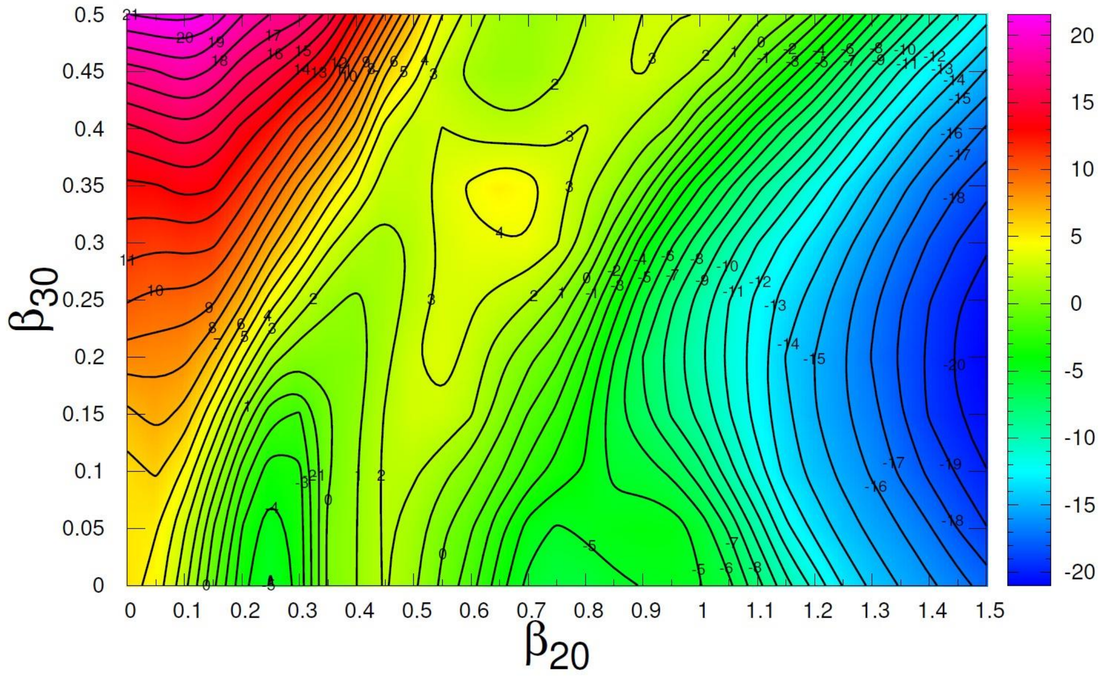

$^{54}Cr + ^{208}Pb$, $l = 0$

-2 neutrons

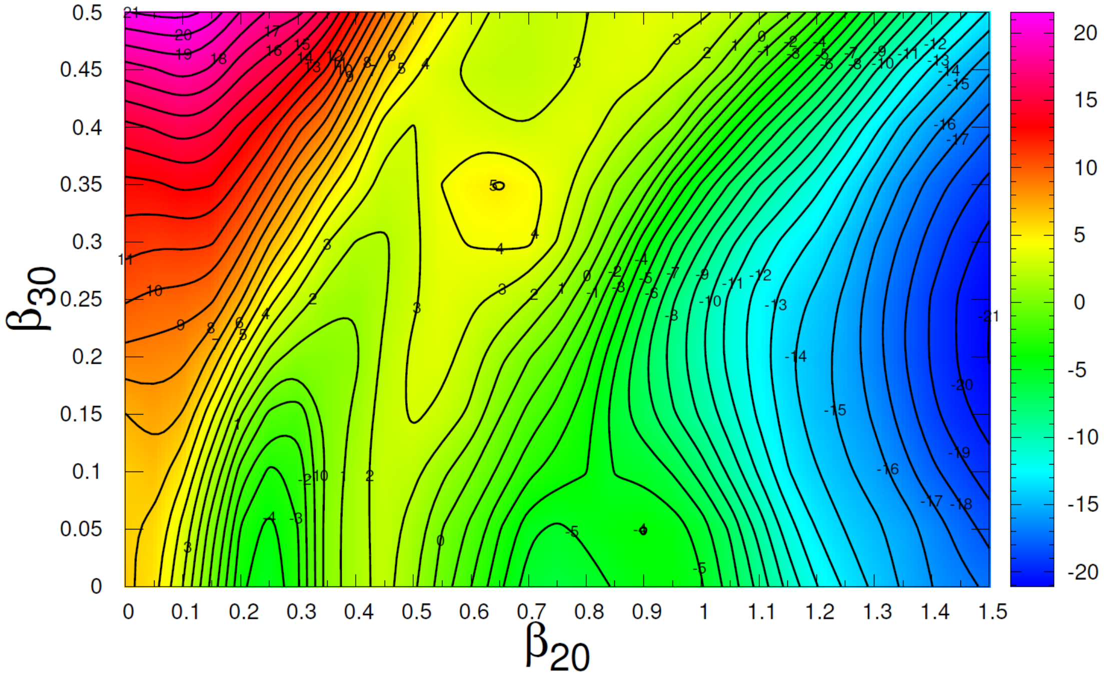

$^{52}Cr + ^{208}Pb$, $l = 0$

Instead of moving only between shapes, we can also change the PESs.

Random walk in fission

- Start in the excited ground state/saddle /second minimum
- Continue the random walk until fission
- Could be used in conjunction with the fusion random walk to describe mass fragment distributions from the fusion-fission process
- Could be used to describe mass fragment distributions from neutron induced fission
- Number of steps is multiple orders of magnitude higher than in fusion, <u>increasing the lower the excitation energy</u>

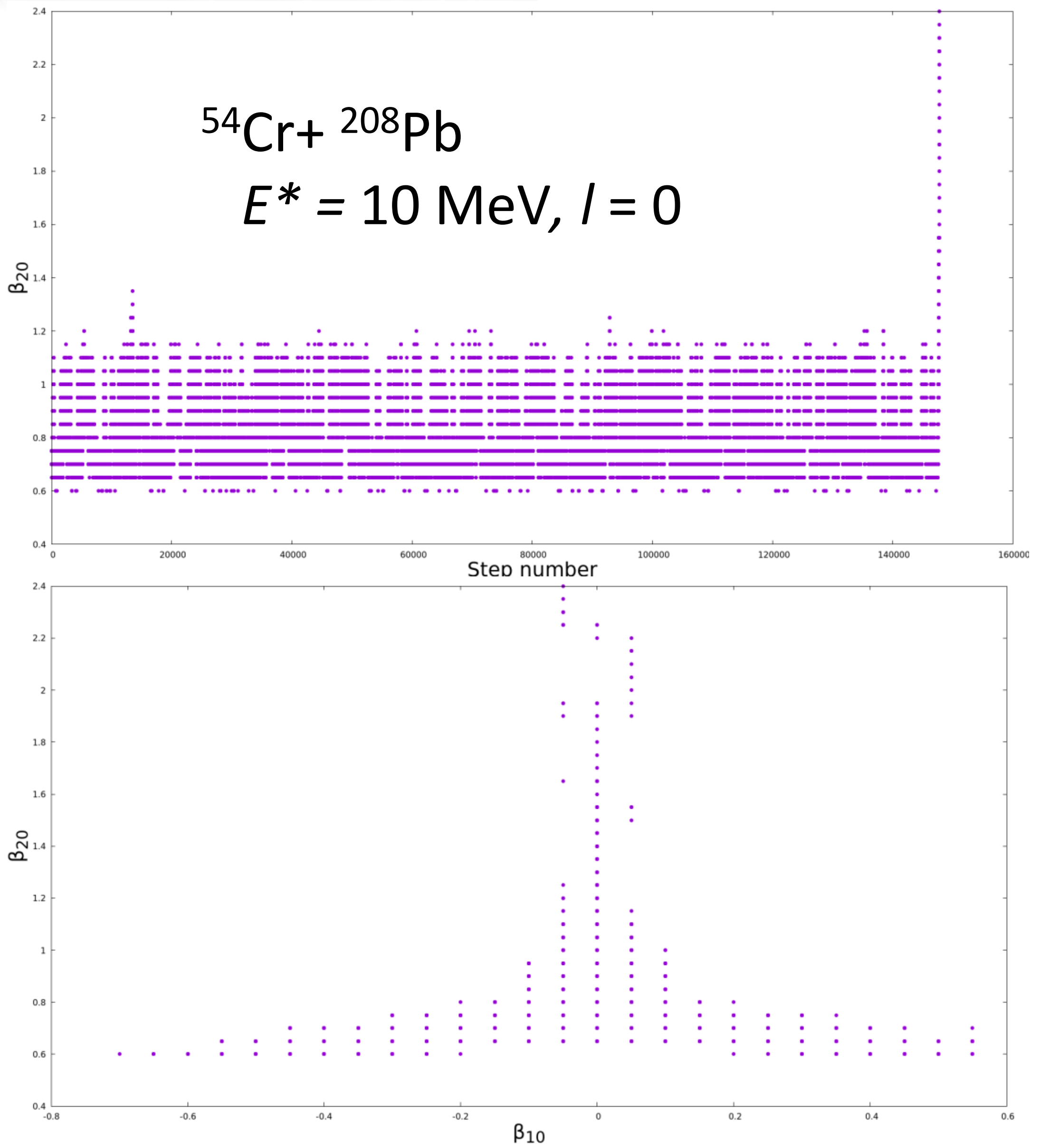

Summary

- The random walk method reproduces experimental results for probability of fusion, even though there are no fitted parameters within the model itself
- Including the β_{10} as an actual shape variable allowed to describe the starting point configuration with only 4 deformation parameters
- The new approach makes possible to predict mass fragment distributions, which can be compared with experimental data
- The random walk method looks to be a promising direction of study, both for fusion and fission of superheavy nuclei

Thank you for your attention!

NATIONAL CENTRE FOR NUCLEAR RESEARCH ŚWIERK

www.ncbj.gov.pl